Trait components of whole plant water use efficiency are defined by unique, environmentally responsive genetic signatures in the model C_4 grass *Setaria*

Max J. Feldman[1], Patrick Z. Ellsworth[2], Noah Fahlgren[1], Malia A. Gehan[1], Asaph B. Cousins[2] and Ivan Baxter[1,3,*]

*Corresponding author
E-mail: ivan.baxter@ars.usda.gov (IB)

[1]Donald Danforth Plant Science Center, St. Louis, Missouri, USA
[2]School of Biological Sciences, Washington State University, Pullman, Washington, USA
[3]USDA-ARS, Plant Genetics Research Unit, St. Louis, Missouri, USA

One sentence summary: Regulation of plant growth can be partitioned into water dependent and water independent processes controlled by unique genetic components.

ABSTRACT

Plant growth and water use are interrelated processes influenced by the genetic control of both plant morphological and biochemical characteristics. Improving plant water use efficiency (WUE) to sustain growth in different environments is an important breeding objective that can improve crop yields and enhance agricultural sustainability. However, genetic improvements of WUE using traditional methods have proven difficult due to low throughput and environmental heterogeneity encountered in field settings. To overcome these limitations the study presented here utilizes a high-throughput phenotyping platform to quantify plant size and water use of an interspecific *Setaria italica* x *Setaria viridis* recombinant inbred line population at daily intervals in both well-watered and water-limited conditions. Our findings indicate that measurements of plant size and water use in this system are strongly correlated; therefore, a linear modeling approach was used

to partition this relationship into predicted values of plant size given water use and deviations from this relationship at the genotype level. The resulting traits describing plant size, water use and WUE were all heritable and responsive to soil water availability, allowing for a genetic dissection of the components of plant WUE under different watering treatments. Linkage mapping identified major loci underlying two different pleiotropic components of WUE. This study indicates that alleles controlling WUE derived from both wild and domesticated accessions of the model C_4 species *Setaria* can be utilized to predictably modulate trait values given a specified precipitation regime.

INTRODUCTION

Improving crop productivity while simultaneously reducing agricultural water input is essential to ensure the security of our global food supply and protect our diminishing fresh water resources. Agriculture is by far the greatest industrial consumer of fresh water, largely because productivity losses related to drought stress can decrease crop yields by greater than 50% (Boyer, 1982; Hamdy et al., 2003). Addressing these challenges will require an integrated approach that combines irrigation practices that minimize water loss and deployment of crop plants with superior water use efficiency (Boutraa, 2010; Davies and Bennett, 2015; Evans and Sadler, 2008; Gregory and George, 2011; Morison et al., 2008; Stanhill, 1986).

Plant water use efficiency (WUE) can be broadly defined as the ratio of biomass produced to total water lost by the plant (Bacon, 2009; Blum, 2009; Condon, 2004; Evans and Sadler, 2008; Monteith, 1993; Morison et al., 2008; Tardieu, 2013). This complex trait is determined by many factors including photosynthetic carbon assimilated per unit of water transpired (Condon et al., 2002; Farquhar et al., 1989; Morison et al., 2008; Penman and Schofield, 1951; Seibt et al., 2008), leaf architecture (Brodribb et al., 2007; Sack and Holbrook, 2006), stomata characteristics (Franks and Farquhar, 2006; Lawson and Blatt, 2014), epidermal wax content (Premachandra et al., 1994), canopy and root architecture (White and

62 Snow, 2012; Martre et al., 2001), stomatal dynamics (Blatt, 2000; Hetherington and
63 Woodward, 2003; Lawson et al., 2010; Flood et al., 2011; Lawson et al., 2012) ,
64 hydraulic transport (Edwards et al., 2012; Holloway-Phillips and Brodribb, 2011),
65 portion of carbon lost from respiration (Escalona et al., 2012; Tomás et al., 2014)
66 and partitioning of photo-assimilate (Carmo-Silva et al., 2009; Chaves, 1991). Given
67 that plant species (Stewart et al., 1995; Winter et al., 2005; Zegada-Lizarazu and
68 Iijima, 2005; Zhou et al., 2012) and ecotypes within species (Kenney et al., 2014;
69 Lopez et al., 2015; Nakhforoosh et al., 2016; Pater et al., 2017; Ryan et al., 2016; Xu
70 et al., 2009) exhibit variation in WUE it is likely that the characteristics which
71 determine this trait are under genetic control and have evolved in response to
72 different environmental conditions such as water availability (Assouline and Or,
73 2013; Brodribb et al., 2009; Huxman et al., 2004). Therefore, WUE is likely
74 influenced by both genetically encoded developmental programs and changes in
75 growth environments throughout the plant lifecycle (Fleury et al., 2010).
76 The technical challenges associated with measuring plant size and
77 transpiration in large structured genetic populations has historically limited
78 experimental efforts aimed at identifying the genetic components associated with
79 WUE. This is particularly difficult in field settings due to year-to-year climate
80 fluctuation and micro-environmental variation observed within agricultural fields.
81 The advent of controlled environment, high-throughput phenotyping instruments
82 (Chen et al., 2014; Fahlgren et al., 2015; Granier et al., 2006; Pereyra-Irujo et al.,
83 2012; Reuzeau et al., 2006; Sadok et al., 2007; Tisné et al., 2013; Walter et al., 2007)
84 alleviates many of these challenges through stringent control of climatic variables
85 and automated, high-resolution measurement of plant size and evapotranspiration
86 across large breeding populations.
87 Evidence from studies conducted on both crop and model plants indicate that
88 the traits associated with WUE are heritable and largely polygenic, although
89 identifying the causal locus associated with differential performance has proven
90 difficult in crop plants due to plant size and genome complexity (Adiredjo et al.,
91 2014; Aparna et al., 2015; Chen et al., 2012; Coupel-Ledru et al., 2016; Honsdorf et

92 al., 2014; Parent et al., 2015; Schoppach et al., 2016; Xu et al., 2009). Utilization of
93 model plants (C_3 annuals *Arabidopsis thaliana* and *Brachypodium distachyon*) that
94 possess tractable genetic and experimental properties has enabled scientists to
95 identify QTL that contribute to WUE (Des Marais et al., 2016; Easlon et al., 2014;
96 Lowry et al., 2013; Mojica et al., 2016; Vasseur et al., 2014), a few of which have
97 been mapped to causal genes (Ruggiero et al., 2017). Species in the genus *Setaria*
98 also possess many of these desirable qualities and can be used as experimental
99 models to identify genetic components associated with WUE in a C_4 plant that is
100 closely related evolutionarily to C_4 crops like maize, sorghum and bioenergy grasses
101 (Bennetzen et al., 2012; Brutnell et al., 2010; Huang et al., 2016; Li and Brutnell,
102 2011; Zhu et al., 2017). However, in order to study the diversity of resource
103 utilization tactics present in natural and mapping populations of *Setaria* (Saha et al.,
104 2016) or other C4 plant species, methods to quantify plant performance and WUE
105 in different environments must be developed.
106 The objectives of this study were to use a controlled environment high-
107 throughput phenotyping system to characterize the genetic architecture of plant
108 size, water use and WUE in an interspecific *Setaria* recombinant inbred population
109 (RIL) under two different watering regimes. Our findings indicate that plant size,
110 water use and WUE are polygenic traits which are influenced by both soil water
111 content and greater than 10 pleiotropic loci whose effect size changes differentially
112 throughout development. In addition, we identify and discuss several aspects of
113 experimental design that should be considered when performing high-throughput
114 phenomics experiments to study plant WUE.
115
116 **MATERIALS AND METHODS**
117 *Plant material and growth conditions*
118 The experiment here was first described in (Feldman et al., 2017), which
119 focused on plant height, and the details are paraphrased here in quotes for clarity.
120 An interspecific *Setaria* F7 RIL population comprised of 189 genotypes (1138
121 individuals) was used for genetic mapping. The RIL population was generated
122 through a cross between the wild-type green foxtail *S. viridis* accession, A10, and the

123 domesticated *S. italica* foxtail millet accession, B100 (Bennetzen et al., 2012; Devos
124 et al., 1998; Wang et al., 1998). After a six-week stratification in moist long fiber
125 sphagnum moss (Luster Leaf Products Inc., USA) at 4°C, *Setaria* seeds were planted
126 in 10 cm diameter white pots pre-filled with ~470 cm^3 of Metro-Mix 360 soil
127 (Hummert, USA) and 0.5 g of Osmocote Classic 14-14-14 fertilizer (Everris, USA).
128 After planting, seeds were given seven days to germinate in a Conviron growth
129 chamber with long day photoperiod (16 h day/8 h night; light intensity
130 230 $\mu mol/m^2/s$) at 31°C day/21°C night before being loaded onto the Bellwether
131 Phenotyping System using a random block design replicating each genotype and
132 treatment combination in triplicate. For each replicate, individual plants of the same
133 genotype were grown side by side with one individual receiving unlimited water
134 supply while the other individual was subjected to water limitation. The growth
135 chamber location of each of these paired replicates was randomly assigned and did
136 not vary during the course of the experiment. Plants were grown on the system for
137 25 days under long day photoperiod (16 h day/8 h night; light intensity 500
138 $\mu mol/m^2/s$) with the same temperature regime used during germination. Relative
139 humidity was maintained between 40 – 80 %. Gravimetric estimation of pot weight
140 was performed 2-3 times per day and water was added to maintain soil volumetric
141 water content at either 33% full-capacity (FC) (water-limited) or 100% FC (well-
142 watered) as determined by (Fahlgren et al., 2015). Prescribed soil water content
143 across both treatment blocks was achieved by 15 days after planting (DAP).
144 The volume of water transpired by individual plants at each pot weighing
145 was calculated as the difference between the measured pot weight and the weight of
146 the pre-filled pot at pot capacity (100% FC) or the difference between current pot
147 weight and the previous weight measurement if no water was added. At the
148 conclusion of each weighing, if the pot weight was below the set point, water was
149 added to the pot to return soil water content back to its target weight. This strategy
150 effectively maintains soil moisture content at a consistent level within both
151 treatment blocks. To evenly establish seedlings before the water limitation
152 treatment began, equal volumes of water (100% FC) were added to all pots for two
153 days after transfer to the system. At 10 DAP, a dry down phase was initiated (no

154 watering) to establish the water-limited treatment block (40% FC) while continuing
155 to maintain a soil water content of 100% FC within the well-watered treatment
156 block.
157
158 *Image acquisition and derived measurements*
159 RGB images of individual plants were acquired using a top-view and a side-
160 view cameras at four different angular rotations (0°, 90° 180°, 270°) every other day
161 at the Bellwether Phenotyping Facility (Fahlgren et al., 2015). Optical zoom was
162 adjusted throughout the experiment to ensure accurate quantification of traits
163 throughout plant development. The unprocessed images and the details of the
164 configuration settings can be found at the following download site:
165 (https://plantcv.danforthcenter.org/pages/data-sets/setaria_height.html).
166 Plant objects were extracted from images and analyzed using custom PlantCV
167 Python scripts specific to each camera (side-view or top-view), zoom level, and lifter
168 height (https://github.com/maxjfeldman/Feldman_Elsworth_Setaria_WUE_2017).
169 Scaling factors relating pixel area and distance to ground truth measurements
170 calculated by (Fahlgren et al., 2015) were used to translate pixels to relative area
171 (pixels/cm^2) and relative distance (pixels/cm).
172
173 *Biomass estimation*
174 At the conclusion of the experiment, 176 individual plants (91 plants from
175 the 100% FC and 85 from the 40% FC) were harvested to measure aboveground
176 biomass. Gravimetric measurement of fresh weight and saturated fresh weight were
177 taken directly upon tissue harvest after which plant tissue was placed into
178 polypropylene micro-perforated bags (PJP MarketPlace #361001), dried for three
179 days at 60 °C and subsequently weighed to determine dry weight biomass.
180 Multivariate linear regression was used to evaluate, select and calibrate a predictive
181 model to estimate both fresh and dry weight plant biomass.
182 Regressing plant fresh weight biomass as a function of side-view area,
183 perimeter length, height, object solidity and width indicated that each of these terms
184 is a significant predictor of fresh weight biomass after stepwise model selection

185 using Akaike's Information Criterion (AIC) (Bozdogan, 1987); multiple $R^2 = 0.89$).
186 Unlike fresh weight biomass, side-view area, width, and height were the only
187 significant terms used for prediction of dry weight biomass after using the AIC
188 stepwise model selection correction procedure (multiple $R^2 = 0.76$). Models
189 containing all significant terms and their interaction achieved a greater model fit,
190 but they introduced artifacts at earlier developmental time points due to model
191 over-fitting (Fig. S1). Generally, models constructed to estimate fresh weight
192 biomass in the well-watered treatment block exhibited greater explanatory power
193 than those constructed to predict dry weight biomass or those in water-limited
194 treatment blocks (Fig. 1).
195 A minimal model containing only the most significant term (side-view area)
196 in both fresh and dry weight models produced a goodness of fit similar to more
197 complex models (fresh weight $R^2 = 0.86$; dry weight $R^2 = 0.74$). To avoid
198 propagation of error, values that incorporated plant fresh weight biomass were
199 calculated based on adjusted side-view pixel area and translated to fresh weight
200 biomass after analysis. Cumulative biomass values calculated on a genotype within
201 treatment basis were interpolated using loess smoothing (Chambers and Hastie,
202 1992). Plant size accumulation on a per day basis was calculated as the difference
203 between the loess fit values on a given day and the estimates from the previous day.
204
205 *Water loss tabulation*
206 The LemnaTec instrument at the Bellwether Phenotyping Facility provided
207 measurements of water use based upon the gravimetric weight of each pot before
208 watering, the volume of water applied, and the resulting weight after watering. On
209 days when the volume of water added to a pot was greater than zero, the daily
210 volume of water added was the sum of water volume added over a single calendar
211 day. On days when water was not added (e.g. during the dry down period), the
212 water volume was calculated as the minimum gravimetric weight of the pot on the
213 day in question subtracted from the minimum weight value from the previous day.
214 The cumulative volume of water used on a specific day was the sum of all water
215 used prior to that day. By fifteen days after planting (DAP), the dry down phase for

216 the water-limited treatment group was complete and pots containing plants lost
217 substantially more water than their empty pot counterparts in the well-watered
218 treatment group (Fig. 1). This observation indicates pot water loss cannot be
219 considered a proximity measure of total plant transpiration before day 15 in this
220 experiment (Fig. 1). Examination of the ratio between fresh weight biomass
221 accumulated relative to the amount of water used and mathematical prediction of
222 the amount of water used per day over this period suggests that the amount of
223 water used between day 15 and 17 can be used as an approximation of cumulative
224 water transpired by the plant throughout this experiment up to this point (Fig. S2).
225 This data and the observation that at day 17 the plants are still relatively small (less
226 than 8% of their maximum size on average) support the rationale of starting the
227 analysis on this day (Fig. 1). Volumes of water use (daily and cumulative) on a
228 genotype within treatment basis were estimated using loess smoothing.
229
230 *Heritability and trait variance partitioning*
231 We used the same approach as in (Feldman et al., 2017) and the details are
232 paraphrased here in quotes for clarity. During this experiment, plant area was
233 measured every other day, so the number of replicates per treatment to calculate
234 broad sense heritability on any given day was limited. To alleviate this technical
235 shortcoming, trait values for each individual were interpolated across missing days
236 using loess smoothing.
237 Variance components corresponding to broad sense heritability and total
238 variance explained was estimated using a mixed linear model using the R package
239 lme4 (Bates et al., 2015). Broad sense heritability was calculated using two
240 methods. Within an individual experiment, broad sense heritability on a line-
241 estimate basis was calculated using the following formula:
242
243 Equation 1:
244 $$H^2_{experiment} = \sigma^2_{genotype} / (\sigma^2_{genotype} + (\sigma^2_{genotype\ X\ treatment} / n_{treatment}) + (\sigma^2_{residual} /$$
245 $$n_{replicates}))$$

246

247 in which $n_{treatment}$ is the harmonic mean of the number of treatment blocks in which
248 each line was observed and $n_{replicates}$ is the harmonic mean of number of replicates of
249 each genotype in the experiment. Heritability within treatment blocks was
250 calculated by fitting a linear model with genotype as the only explanatory factor
251 within each treatment block.

252

253 Equation 2:

254 $$H^2_{\text{treatment block}} = \sigma^2_{\text{genotype}} / \sigma^2_{\text{total variance}}$$

255

256 The proportion of variance attributed to genotype divided by total variance
257 within each treatment block is reported as broad sense heritability within treatment
258 (equation). Total variance explained was calculated by fitting a linear model
259 including factors, genotype, treatment, plot and genotype x treatment effects across
260 all phenotypic values in all treatments. The proportion of variance that is
261 incorporated into these factors divided by the total variance in the experiment is
262 reported as total variance explained for each factor.

263

264 *QTL analysis*

265 We used the same approach as in (Feldman et al., 2017) and the details are
266 repeated here in quotes for clarity. "QTL mapping was performed at each time point
267 within treatment blocks and on the numerical difference, relative difference and
268 trait ratio calculated between treatment blocks using functions encoded within the
269 R/qtl and funqtl package (Broman et al., 2003; Kwak et al., 2016). The functions
270 were called by a set of custom Python and R scripts
271 (https://github.com/maxjfeldman/foxy_qtl_pipeline). Two complimentary analysis
272 methods were utilized. First, a single QTL model genome scan using Haley-Knott
273 regression was performed to identify QTL exhibiting LOD score peaks greater than a
274 permutation based significance threshold ($\alpha = 0.05$, $n = 1000$). Next, a stepwise
275 forward/backward selection procedure was used to identify an additive, multiple

276 QTL model based upon maximization of penalized LOD score. Both procedures were
277 performed at each time point, within treatment blocks and on the numerical
278 difference relative difference and trait ratio calculated between phenotypic values
279 measured in treatment blocks at each time point. QTL associated with difference or
280 ratio composite traits may identify loci associated with genotype by environment
281 interaction (Des Marais et al., 2013).
282 The function-valued approach described by (Kwak et al., 2016), was used to
283 identify QTL associated with the average (SLOD) and maximum (MLOD) score at
284 each locus throughout the experiment. Each genotypic mean trait within treatments
285 was estimated using a logistic function, and the QTL significance threshold was
286 determined based upon permutation-based likelihood of observing the empirical
287 SLOD or MLOD test statistic. Separate, independent linkage mapping analysis
288 performed at each time point identified a larger number of QTL locations relative to
289 similar function valued analysis based on the SLOD and MLOD statistics calculated
290 at each individual marker throughout the experimental time course.
291 After refinement of QTL position estimates, the significance of fit for the full multiple
292 QTL model was assessed using type III analysis of variance (ANOVA). The
293 contribution of individual loci was assessed using drop-one-term, type III ANOVA.
294 The absolute and relative allelic effect sizes were determined by comparing the fit of
295 the full model to a sub-model with one of the terms removed. All putative protein
296 coding genes (*Setaria viridis* genome version 1.1) found within a 1.5-logarithm of
297 the odds (LOD) confidence interval were reported for each QTL."
298
299 **RESULTS**
300
301 *Measuring plant size and water use throughout the plant lifecycle*
302 Recurrent measurement of plant size and water use was performed on
303 individuals of a *Setaria* recombinant inbred population (Devos et al., 1998; Devos et
304 al., 1998) grown at two soil water content levels at the Bellwether Phenotyping
305 Facility (Fahlgren et al., 2015). Images of each individual plant were captured every
306 other day from 7 to 33 days after sowing and plant objects were isolated and

Figure 1. Plant size and water use can be accurately inferred throughout a majority of the plant life cycle. A) Significant correlations between plant fresh weight and pixel area were observed in both the well-watered and water-limited treatment blocks. B) Plants exhibited a sigmoidal growth curve, characterized by an average maximal rate of growth between 23– 26 days after planting. Green lines reflect absolute average size, whereas purple lines report on growth rate. Dark and lighter shaded lines report the well-watered and water-limited treatment blocks respectively. C) Daily water loss can be accurately measured at 17 days after planting. Dark blue and orange lines correspond to average daily water lost from pots, whereas the lines with lighter shades of similar colors report the average water loss of empty pots. The dashed black line denotes the day at which dry down within the water-limited treatment block is complete whereas the dashed red line demarks when water use can be accurately measured. D) By 17 days after planting, plants have attained less than 8% of their total biomass.

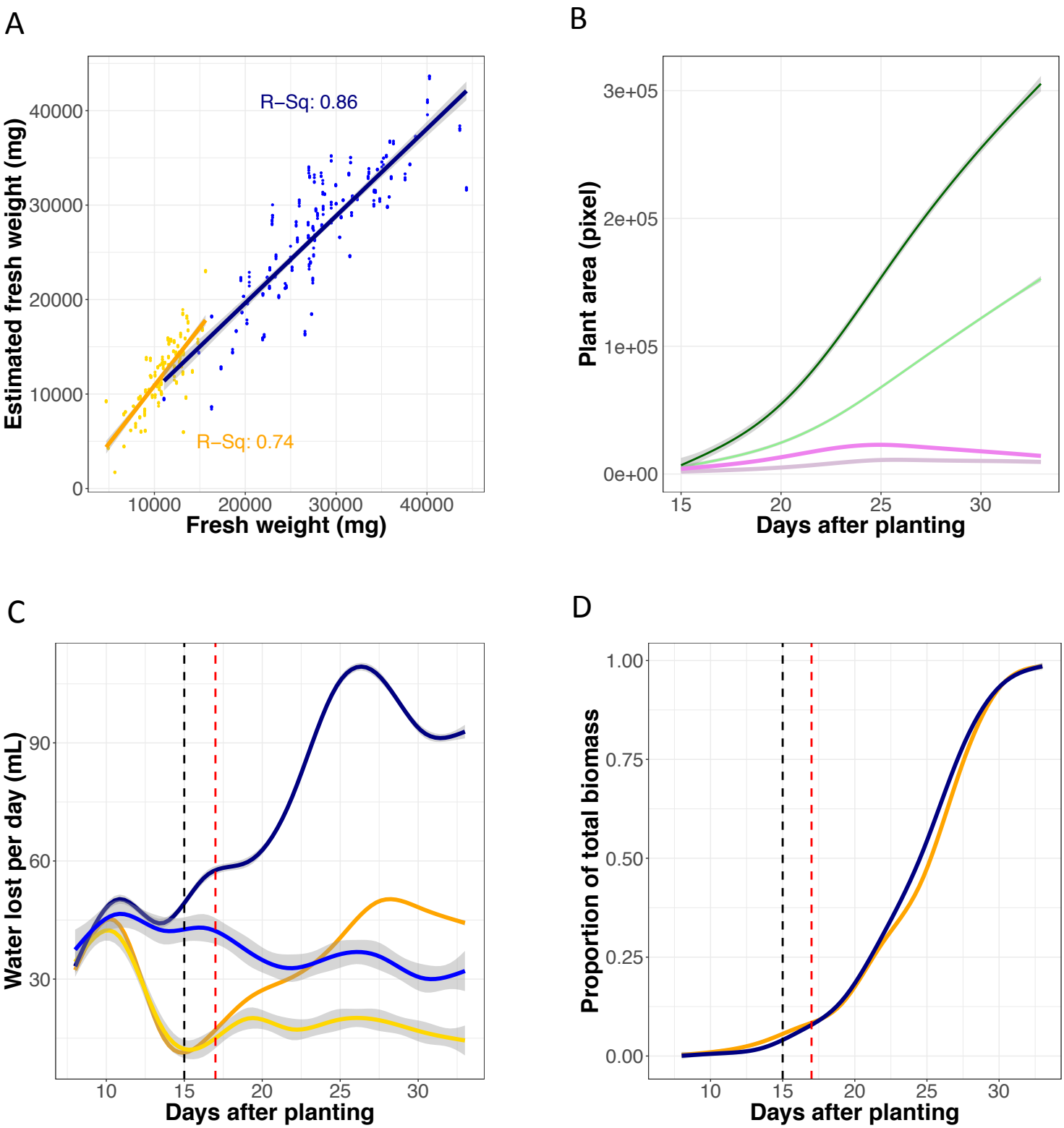

quantified using PlantCV (Fahlgren et al., 2015; Feldman et al., 2017). Weight estimates of fresh and dry-weight aboveground biomass were calculated using a simple linear model featuring side-view area as the only predictor (Fig. 1, Fig. S3).

Daily plant water use was inferred through gravimetric measurement of pot weight performed two to three times each day by the LemnaTec instrument. The amount of water used by individual plants was calculated as the difference between the measured weight of the pot and the weight of a pre-filled pot at a fixed point that is proportional to its water holding capacity (100% FC) or the difference between current weight and the previous weight measurement if no water was added. At the conclusion of each weighing event, if pot weight was below the set point, water was added to the pot to return it to the target weight value. This strategy effectively maintains soil moisture potential at a consistent level within both treatment blocks. To evenly establish seedlings before the water limitation treatment, equal volumes of water (100% FC) were added to all pots for two days after transfer onto the system. At 10 days after sewing, a dry down phase was initiated (no watering) to establish uniformity within the water-limited treatment block (40% FC) while continuing to maintain a soil water content of 100% FC within the well-watered treatment block.

Examination of water loss from empty pots relative to those containing plants suggested that early in the experiment a majority of water loss was exclusively due to evaporation from the soil surface and did not informatively report on plant transpiration (Fig. 1) (Ge et al., 2016). Beginning the analysis at day 17 enabled us to minimize the artifacts of evaporation that dominated early in the experiment while still capturing growth attributes over a large proportion (~92%) of the plant growth within the experiment (Fig. 1). Another potential confounding issue was the use of a fixed set point for the pot weight, which neglected the increasing weight of the plant when calculating the amount of water needed to return the pot weight to the set point during watering jobs. This decreased the volume of water present within each pot after watering by approximately 12.5% (well-watered) and 17.5% (water-limited) on average by the end of the experiment (Fig. S4).

Figure 2. Plant size and water use are tightly correlated.
Pearson Correlation Coefficient both within (blue is well-watered, orange is water-limited) and between (red is across both) treatment blocks indicates strong correlation between these two characteristics, although the correlation between the rate of plant growth and daily water use decreases as plants approach maximum size. A) Correlation between cumulative plant size and water use. B) The relationship between plant size and water use at 20, 25 and 30 days after planting. C) Correlation between the rate of plant growth and daily water use. B) The relationship between plant growth rate and daily water use at 20, 25 and 30 days after planting.

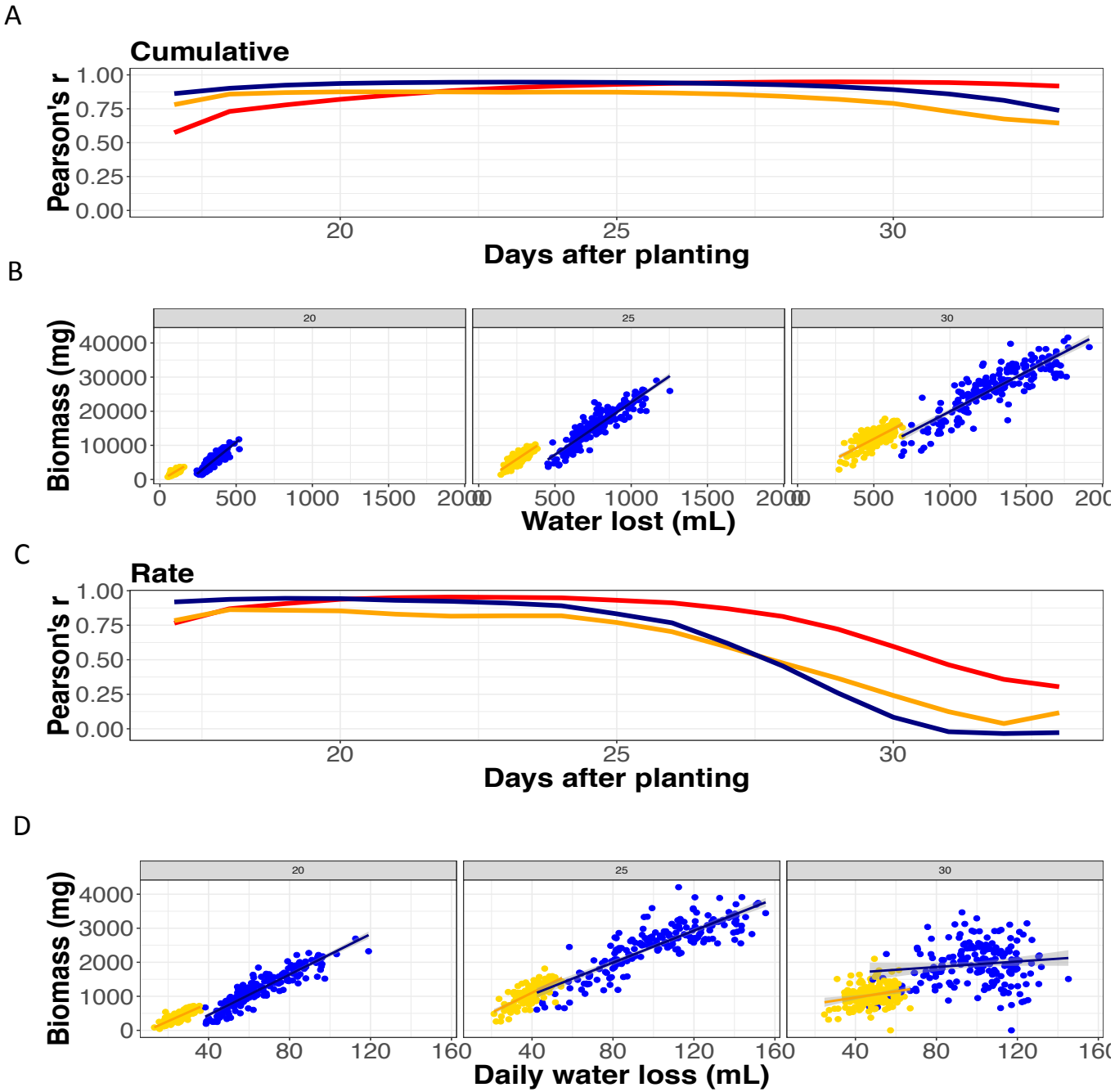

338 Loess smoothing was used to interpolate the values of traits on a genotype
339 level within each treatment block across all experimental time points (Chambers
340 and Hastie, 1992). Fitting of parametric models was avoided because in many cases
341 the trait values exhibited genotype specific temporal responses that could not be
342 accurately represented by a single model type across the entire population. Rate
343 statistics were calculated from these loess smoothed estimates as the difference of
344 the trait between days. Plots illustrating the mean and variance of each trait can be
345 observed in FIG. S5.
346
347 *Plant size and water use are correlated*
348 Over the course of this experiment cumulative plant size and water use were
349 highly correlated. Correlation was tightest between 21 and 27 DAP in the well-
350 watered treatment block (> 0.94) and quite strong between 20 and 27 DAP in the
351 water-limited treatment block (> 0.87, Fig. 2). In both treatment blocks, correlations
352 between these characters were weakest at the beginning and end of the experiment
353 but never dropped below 0.67. The correlation of the rate statistics associated with
354 these traits appeared qualitatively different. Correlation between plant growth rate
355 and the rate of water use was initially strong (> 0.79) but rapidly decreased at about
356 26 DAP as the rate of growth slowed (ultimately approaching zero) by the end of the
357 experiment (Fig. 2) while transpiration remained high.
358 We implement two numerical approaches to characterize the genetic
359 architecture of the relationship between these traits. The first method, which is
360 hereafter referred to as the water use efficiency ratio (WUE_{ratio}), calculated the ratio
361 of biomass relative to the volume of water lost from the pot. This calculation was
362 performed on a cumulative or daily rate basis.
363
364 Equation 3:
365 WUE_{ratio} (pixel/mL) = plant size (pixel) / plant water lost (mL)
366
367 Values of cumulative WUE_{ratio} calculated during this experiment were
368 comparable to other experiments where plant size and water use was measured

Figure 3. Modeling the relationship between plant size and water use results in two traits. This approach results in predicted value of water use given size (WUE_{fit}) colored in dark blue and deviations from this relationship ($WUE_{residual}$) plotted in red. Plot illustrates this relationship at 30 days after planting.

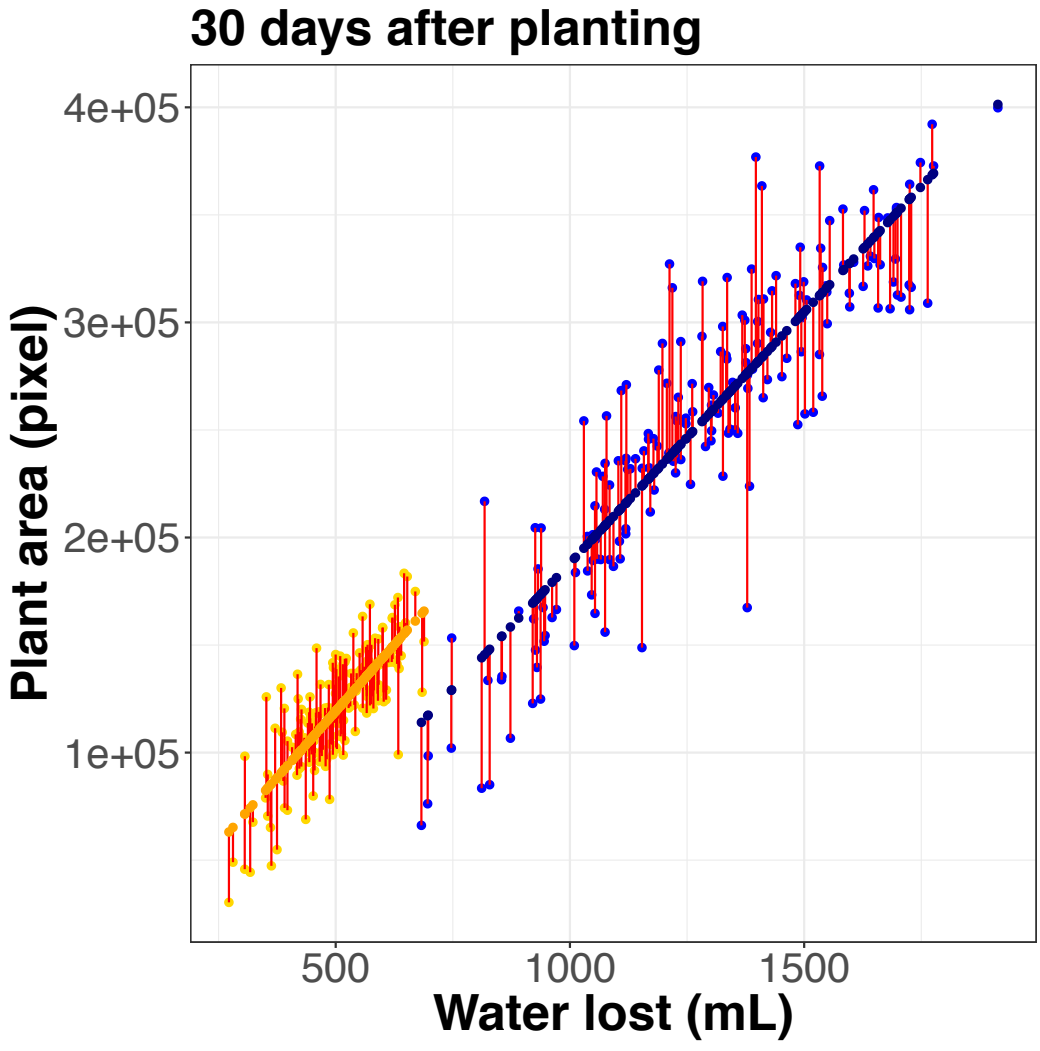

manually at lower throughput (25-29 grams fresh weight / Liter of water, 7-9 grams dry weight / Liter of water). On average, the cumulative and daily rate WUE_{ratio} was greater in the water-limited treatment block than in well-watered conditions. In principle, the WUE_{ratio} should attenuate the relationship between biomass and water use, but significant correlation was still observed between these two variables, particularly within the rate statistic over the last week of the experiment (Fig. S6, Fig. S7).

The high correlation between plant size and water use suggests that they were not independent traits in this experimental setup. Therefore, as a second approach, ordinary least squares linear regression was used to model the relationship between plant biomass and water use. For each day of the experiment, within treatment blocks a WUE_{model} was used to predict plant size (dependent/response variable) based upon water loss (independent/explanatory variable) (Fig. 3). The residual of this model fit was evenly distributed around zero across the entire distribution of the predicted values suggesting minimal bias of this approach (Fig. S8).

Equation 4:

WUE_{fit} (pixel/mL) = plant size (pixel) ~ water lost (mL) + $WUE_{residual}$ (pixel/mL)

This approach resulted in two traits: The first was the predicted model fit (WUE_{fit}) that described the sum of squares relationship between biomass and water use. The residual of this model ($WUE_{residual}$) can be thought of as genotype-specific deviation from this relationship combined with measurement error. As expected, the correlation between the fit values derived from the WUE_{model} was highly correlated with plant size (Fig. S9). A slight correlation between cumulative plant biomass and the residual of the WUE_{model} was observed particularly later in the experiment demonstrating that biomass had components that were not accounted for by the linear model fit (Fig. S10). Varying the dependence structure/assignment or fitting of the model using major axis regression framework (Legendre, 2014) had little effect on downstream analysis.

400 Each trait (biomass, water loss, WUE_{ratio}, WUE_{fit} and $WUE_{residual}$) exhibited
401 high average heritability over all experimental time points within and across
402 treatment blocks (0.28 – 0.77) (Fig. S11). Heritability tended to achieve its
403 maximum value in the middle of the experiment with decreased heritability
404 observed at the beginning and the end of the study. Proportionally, the treatment
405 effect of water limitation explained the largest percentage of variance within
406 biomass, water loss and the WUE_{fit} although genotype and genotype x treatment
407 interaction also explain a substantial margin of the variance (Fig. S12). Heritability
408 of the rate traits was generally similar but on average 5% lower than the heritability
409 of the cumulative traits. In all cases, the average heritability of each trait was greater
410 within the well-watered treatment block relative to the value calculated in water-
411 limited treatment block.
412
413 *The genetic architecture of plant size and water use traits*
414 For each day of the experiment, a best fit multiple QTL model was selected
415 for each trait (plant size, water use, WUE_{ratio}, WUE_{fit} and $WUE_{residual}$) and the daily
416 rate of change of the trait within each treatment block based upon penalized LOD
417 score using a standard stepwise forward/backward selection procedure (Broman et
418 al., 2003). This approach identified 86 (cumulative Fig. 4; Table S1) and 106 (rate
419 Fig. S13; Table S1) unique SNPs associated with at least one of the five traits. Many
420 of these uniquely identified SNP positions group into clusters of tightly linked loci
421 that are likely representative of a single QTL location. These local clusters of SNPs
422 (10 cM radius) were then condensed into the most significant marker within each
423 cluster to simplify comparisons of genetic architecture between traits (Fig. S13; Fig.
424 S14). Collapsing these SNP positions yielded 23 unique QTL locations associated
425 with cumulative trait values (Fig. 5) and 27 unique rate QTL locations (Table S2).
426 Of the 23 unique QTL identified, plant biomass contributes the largest
427 proportion of QTL to this set (18) followed by WUE_{ratio} (12), WUE_{fit} (11), $WUE_{residual}$
428 (10) and water lost (8) (Fig. 5, Fig. S16). Despite the fact that only one QTL location
429 (2@96) was common across all traits and environments, the genetic architecture
430 that contributes to each of these characteristics was clearly related. The strong

Figure 4. Eighty-six unique QTL locations were detected across all traits in this experiment. Each box corresponds to an individual chromosome, where the values along the x-axis are chromosome position and values along the y-axis denote the proportion of genetic variance explained by the QTL. Each triangle represents a single QTL detected, where the color indicates the trait each QTL is associated with (green = plant size, blue = water use, orange = WUE_{ratio}, black = WUE_{fit}, red = $WUE_{residual}$). The darkness of color shading is indicative of treatment block where darker represents well-watered and lighter corresponds to the water-limited block respectively. The direction of the arrow indicates the directional effect of the B100 parental allele.

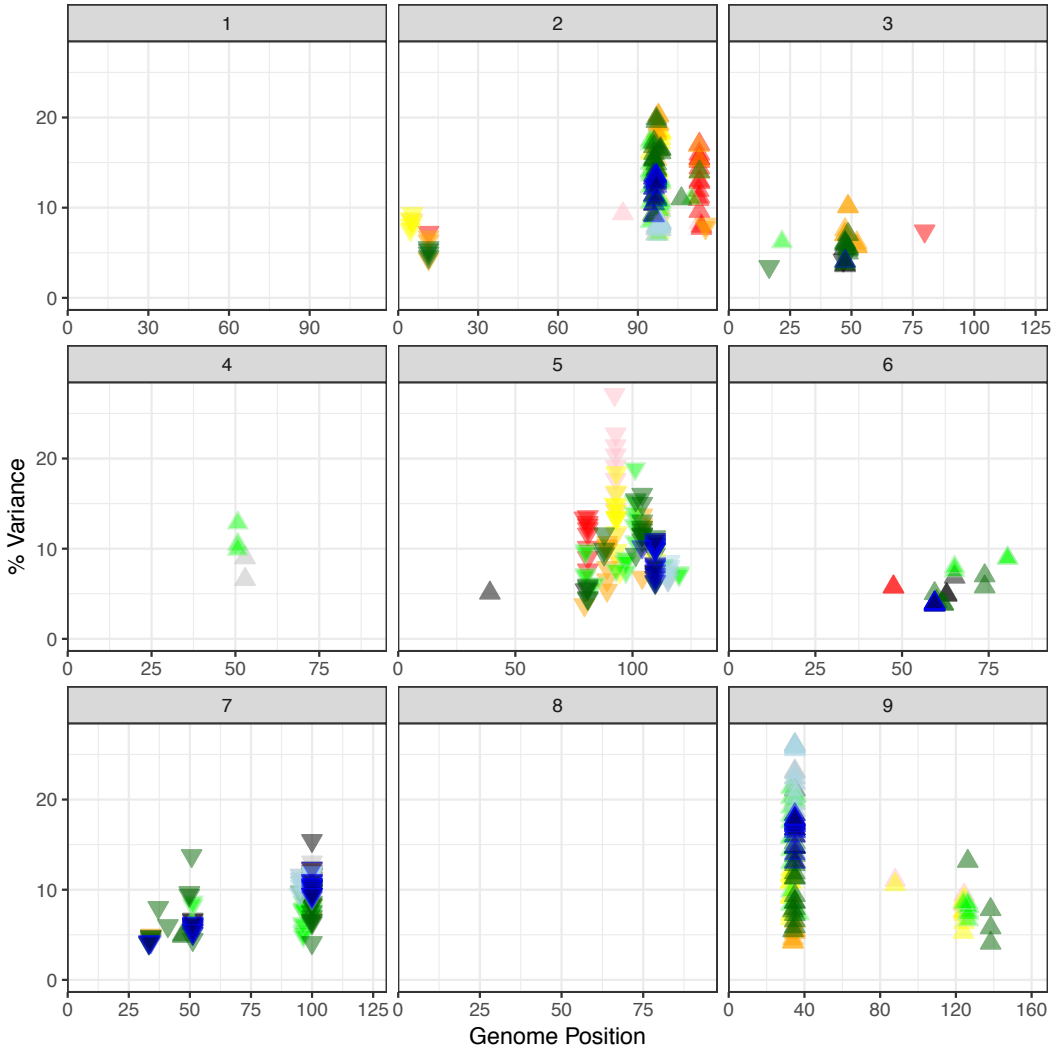

Figure 5. The genetic components that contribute to subsets of traits largely overlap.
The QTL locations identified are plotted on the x-axis and the traits are plotted on the y-axis. Colored matrix entries denote at least one significant association within this experiment. A) The genetic architecture of cumulative traits. B) The genetic loci associated with trait rate of change. C) Genetic components associated with genotype x environment traits.

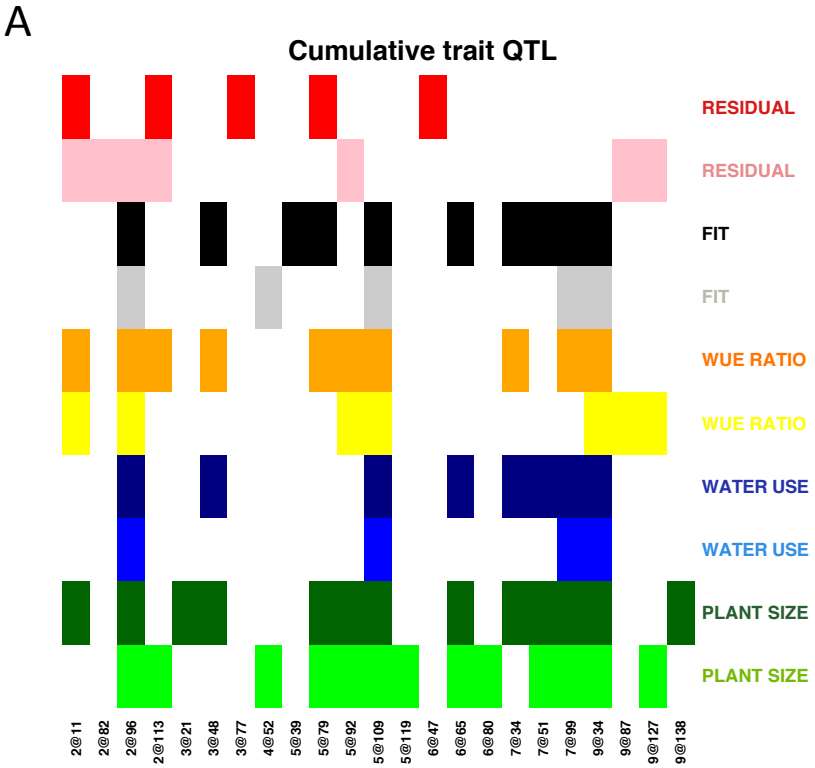

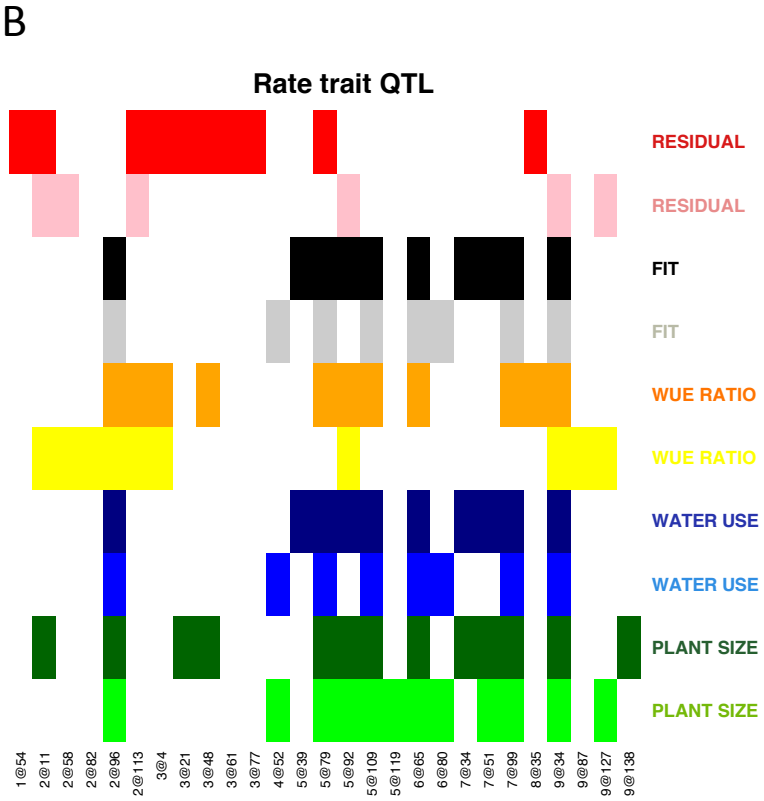

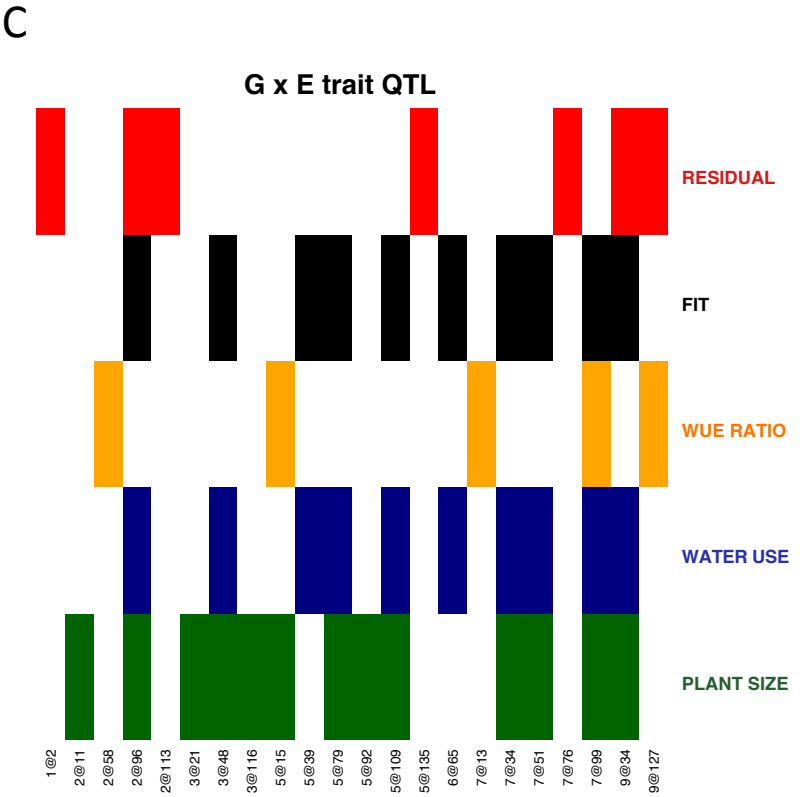

431 correlation of plant size and water loss with the predicted value of plant size given
432 water loss (WUE_{fit}) are clearly reflected within the genetic architecture associated
433 with these traits. Plant size, water loss and WUE_{fit} all shared 8 QTL (2@96, 3@48,
434 5@109, 6@65, 7@34, 7@51, 7@99 and 9@34) either within the well-watered or
435 water-limited treatment block (Fig. 5, Fig. S16). Plant size, WUE_{ratio} and deviations
436 from the relationship between plant size and water use ($WUE_{residual}$) shared five QTL
437 unique to this subset (2@11, 2@113, 5@79, 5@92, and 9@127) which enable
438 divergence from the fundamental relationship between plant size and water loss
439 (Fig. 5, Fig. S16). Several QTL were identified as being uniquely associated with
440 plant size (3@21, 5@119, 6@80, 9@138), $WUE_{residual}$ (2@82 3@77, 6@47) and
441 WUE_{fit} (5@39) whereas no QTL were identified as being uniquely associated with
442 water loss or WUE_{ratio} (Fig. 5, Fig. S16).
443 The genetic architecture of all five traits appears to be influenced by water
444 availability. All traits other than water loss exhibited QTL unique to each treatment
445 block (Fig. 5, Fig. S17). Biomass, water lost, and WUE_{fit} all shared four QTL in
446 common across environments (2@96, 5@109, 7@99 and 9@34) where as WUE_{ratio}
447 and the $WUE_{residual}$ shared a single QTL (2@11) between blocks not found associated
448 with the other traits. Two QTL (3@48, 7@34) were found specifically within the
449 well-watered treatment block for all traits other than $WUE_{residual}$ whereas QTL
450 specific to water-limited environment identified common QTL associated with
451 biomass and WUE_{fit} (4@52) or WUE_{ratio} and $WUE_{residual}$ (9@87, 9@127).
452 The identity of QTL associated with the daily rate values suggest that the
453 genetic architectures were largely cognate with the QTL associated with the traits
454 themselves, both in identity and response to treatment. In total, 28 QTL comprised
455 the union of all unique QTL associated with both the trait value and the daily rate of
456 change calculated from the trait value. Of these QTL, 22 were common between both
457 the trait value and rate statistic associated with the trait, whereas five are only
458 found associated with the rate (1@54, 2@58, 3@4, 3@61, 8@35) and only one QTL
459 was uniquely associated with the cumulative trait values alone (6@47) (Fig. S18).
460
461 *Genotype x environment interactions*

462 To assess the genetic architecture of genotype x environment interactions,
463 mapping was performed on numerical difference, relative difference and trait ratio
464 between the phenotypic values observed within each treatment block. In total, 148
465 unique SNP locations were identified as being significantly associated with at least
466 one of the difference trait formulations across all standard and derived plant size
467 and water use traits (Table S3). Substantial overlap between these categories of
468 genotype x interaction traits indicates that each formulation detects similar genetic
469 signals (Fig. S19) although the large number SNPs found uniquely associated with
470 the trait ratio may indicate that some of these associations may be spurious. As such,
471 these QTL (trait ratio genotype x environment QTL) were removed from further
472 analysis. The numerical difference and relative difference traits exhibited
473 association with 43 and 40 unique SNP positions, which were representative of 20
474 and 18 QTL respectively (Table S4, Fig. S20-22).
475
476 A majority of the QTL (10/15) identified as being associated with the trait
477 difference between treatment blocks were also found associated with the
478 cumulative trait in both treatment blocks (Fig. 5). The exceptions to this were QTL
479 located on 3@21, 3@48, 5@39, 7@34 and 9@127 that were identified as being
480 significantly associated with the difference between treatment blocks but only
481 identified in either well-watered (3@21, 3@48, 5@39, 7@34) or water-limited
482 conditions (9@127). Interestingly, the QTL located on 3@48, 7@34 and 9@127
483 were associated with more than one trait in a single treatment block which may
484 indicate that these QTL impart pleiotropic phenotypic effects that were dependent
485 upon soil water content (Fig. 5).
486
487 *The temporal genetic architecture of plant growth and water usage*
488 In order to account for the time dependence of the traits for the five plant
489 traits, we used a function-valued approach based upon average log-odds score
490 throughout across the experiment (SLOD) for each trait (Kwak et al., 2016). This
491 analysis parallels the individual time point analysis, although the reduction of

Figure 6. Significant associations identified using single marker scan functional QTL mapping. Chromosomal position is plotted on the x-axis whereas LOD score of trait association across the genome is plotted on the y-axis. Treatment block is indicated by color intensity (darker is well-watered and lighter is water-limited). Significance thresholds (based on 1000 permutations) are plotted as dashed yellow (water-limited) and red (well-watered) lines respectively.

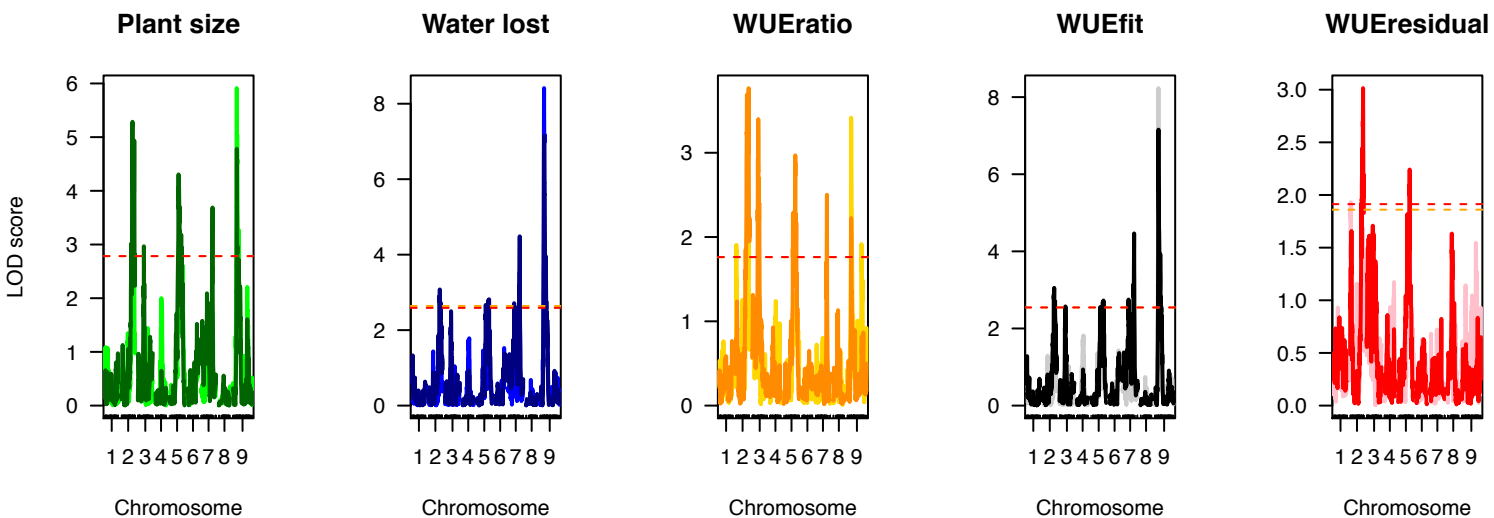

492 complexity (fewer, higher confidence QTL) provides an opportunity for
493 simplification and better understanding of the major loci that influence plant WUE.
494 SLOD based function-valued QTL models indicate that several major QTL
495 (2@96, 5@109, 7@99, and 9@36) influenced both plant size and water use related
496 traits, although the magnitude of statistical significance attributed to each loci
497 varied by trait and throughout plant development (Fig. 6, Fig S23). Using the SLOD
498 approach, we were able to partition combinations of QTL unique to related traits
499 (Fig. 6). For several QTL (those around 2@96 and 5@109) the positional location at
500 which maximal LOD score was observed changed noticeably in a trait and
501 environment dependent manner either due to multiple closely linked loci or noise in
502 our measurements. Because the confidence intervals of the QTL generally overlap,
503 our reporting in this section will hereafter refer to these loci by their approximate
504 chromosomal location.
505 Both plant biomass and cumulative water use exhibited almost a complete
506 overlap of QTL within the well-watered treatment block, whereas plant size given
507 water use (WUE_{fit}) and deviation of plant size from this fundamental relationship
508 ($WUE_{residual}$) each exhibit a unique genetic signature (Fig 6). As observed when trait
509 values at individual time points were treated as independent traits, a single QTL on
510 2@96 is the only genetic component that was shared across all five traits. The linear
511 modeling approach successfully partitions out QTL associated with WUE_{fit} (2@96,
512 7@99, 9@36) from the genetic components that contribute to deviations from the
513 plant size ~ water use relationship ($WUE_{residual}$; 2@96, 5@109). The QTL associated
514 with the WUE_{ratio} (2@96, 3@52, 5@109) also likely reflects deviations from the
515 relationship between biomass given water loss associated with the $WUE_{residual}$.
516 Overall, the identity of QTL associated with each trait was largely identical between
517 the two treatment blocks (Fig. 6, Fig. S23) as were the QTL associated with the
518 values of rate statistics derived from these measurements (Fig. S24, stepwise
519 method; Fig. S25, scanone method).
520
521 *A temporal model of the genetic architecture that influences plant water use efficiency*

522 Our QTL results suggest at least two components of water use efficiency with
523 distinct genetic architectures. In order to compare the genetic architecture across all
524 traits, treatments and time points in a common framework, we analyzed how each
525 trait was influenced by a common set of loci. Fourteen QTL were selected based
526 upon their association with multiple traits, robust linkage with a single trait and/or
527 having differential contribution to traits across treatment blocks (Table S5) and the
528 proportional contribution of each locus to the additive genetic variance was
529 calculated using drop-one-term, type III, ANOVA performed for all experimental
530 traits, time points and treatment. Agglomerative hierarchical clustering of the
531 signed proportion of additive genetic variance explained by each locus was
532 performed to identify modules of traits and loci that define plant phenotypes.
533 Examination of scree plots of the within group sum of squares suggested that the
534 variance within traits could be attributed to approximately six groupings although a
535 majority of this variance could be captured within the largest 2-3 partitions (Fig.
536 S26). These partitions represented the major relationships between trait classes.
537 The WUE_{ratio} and $WUE_{residual}$ were generally grouped separately from a larger cluster
538 of traits that included cumulative plant size, water use and WUE_{fit} (Fig. 7). The
539 genetic architecture of plant water use and WUE_{fit} were more related to each other
540 than they were to plant size, which formed the third group. The influence of water
541 availability on these traits was apparent from the grouping of clusters whereas the
542 effects of time were clear but distributed within the treatment blocks. The genetic
543 architecture of the WUE_{ratio} in the well-watered treatment block at early time points
544 was more similar to the architecture of plant area than itself later in development
545 whereas plant area in the water-limited treatment block exhibited a genetic
546 architecture similar to the WUE_{ratio} late at the end of the experiment.
547 Examination of the signed, proportional allelic effects within the greater fixed
548 QTL model indicated that QTL on 2@96, 5@109, 7@99 and 9@34 contribute
549 medium-to-large effects on a majority of the traits examined in both treatment
550 blocks (Fig. 8). The B100 allele associated with QTL on 2@96 and 9@34 both
551 contributed to increased plant size, water loss, WUE_{fit} and WUE_{ratio}. The QTL on
552 2@96 exhibited its greatest influence in the well-watered treatment block whereas

Figure 7. Agglomerative hierarchical clustering defines the relationship between plant size, water use and derived water use efficiency traits.
The additive effect size of fourteen common QTLs was calculated across all traits, treatments and developmental time points through hierarchical clustering using Ward's method. Color bars on the bottom indicate trait (green = plant size, blue = water use, orange = WUE_{ratio}, black = WUE_{fit}, red = $WUE_{residual}$), treatment block (blue = well-watered, orange = water limited), and days after planting (grey scale values where white represents the trait on day 17 and black indicates the trait on day 33).

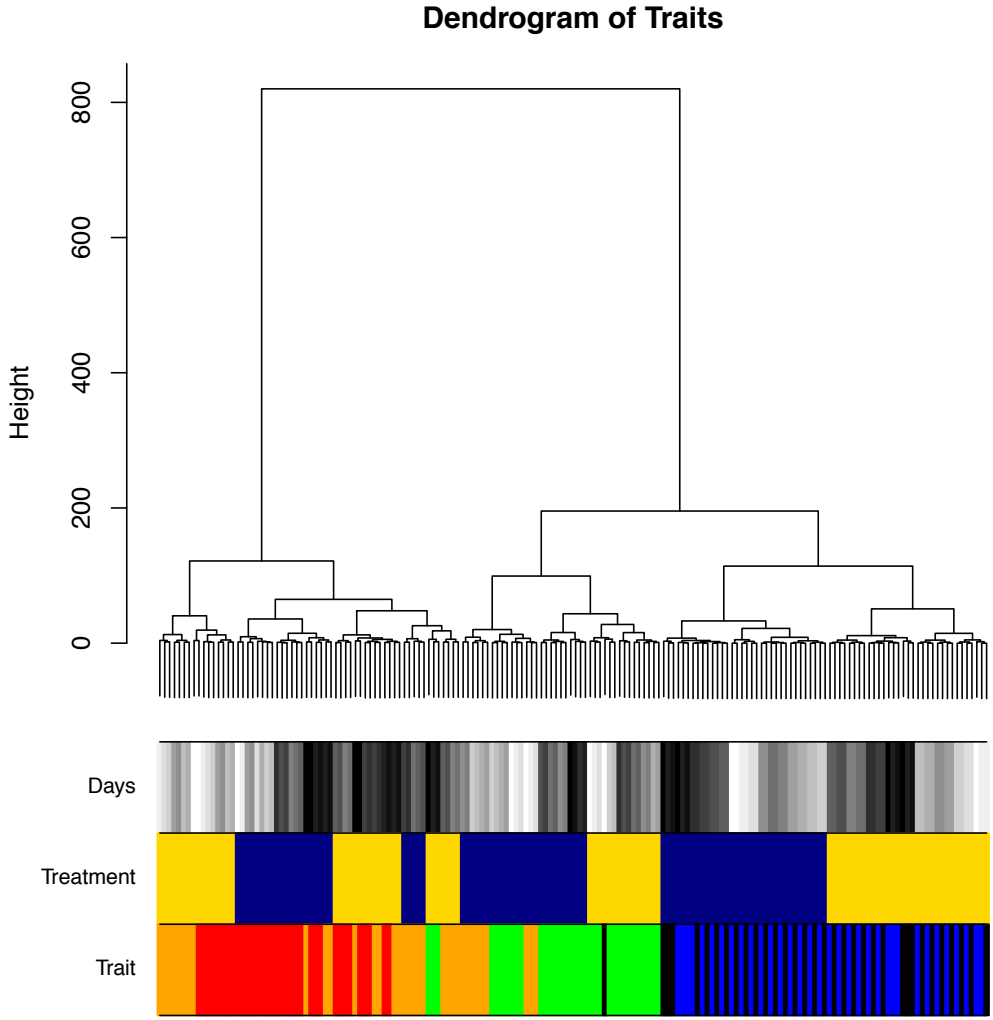

Figure 8. Additive relative effect size of the four major pleiotropic QTL plotted throughout the course of the experiment.

A model containing fourteen QTL was fit across traits, treatment blocks and days. The developmental time point (days after planting) is indicated by the x-axis whereas the proportional additive genetic effect size of the B100 allele is plotted along the y-axis. Columns are representative of traits (green = plant size, blue = water use, orange = WUE_{ratio}, black = WUE_{fit}, red = $WUE_{residual}$) while rows correspond to individual QTL. Shading within the colors denotes treatment block (darker = well-watered, lighter = water-limited).

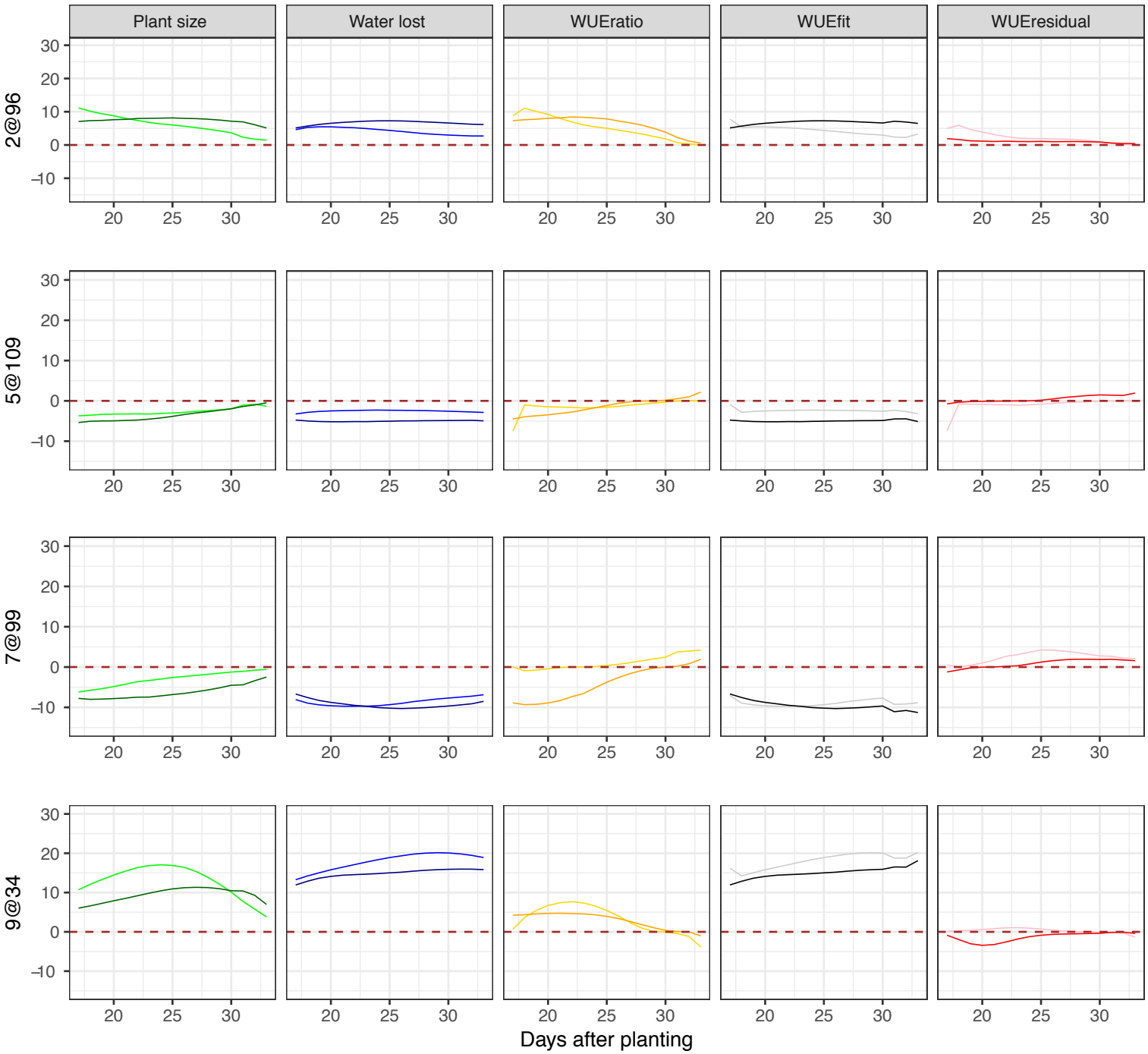

553 the contribution of 9@34 was greater on average in the water-limited treatment
554 block. Both QTL exhibited similar temporal patterns, showing an earlier effect on
555 plant size and WUE_{ratio} but a consistent effect across water loss. Contribution of the
556 B100 allele on 7@99 and 5@109 decrease plant size, water use and the WUE_{fit}
557 traits; the effect of which was greater in well-watered conditions. The magnitude of
558 effects contributed by QTL on 7@99 on plant size decreased through time whereas
559 the effects on water loss and WUE_{fit} peaked after 20 days and decreases slightly
560 thereafter. The 5@109 locus behaves similarly with little temporal variation in
561 plant water use and WUE_{fit}. A majority of the other QTL contributed minor effects
562 that became more prominent in one of the two treatment blocks or at a particular
563 developmental time points. Inheriting the B100 allele at QTL on 2@113, 3@48,
564 4@52, 6@65 and 9@127 increased the values while the B100 allele at the remaining
565 loci (2@11, 5@79, 5@95, 7@34 and 7@53) decreased the value of the traits (Fig.
566 S27).
567 A majority of the QTL exhibit unidirectional effects across both the well-
568 watered and water-limited treatment blocks although the direction of the effect was
569 largely dependent on the trait (Fig. S28). The exceptions to this trend represent
570 short periods of experimental time at which the relative effect size is near zero
571 within one or both treatment blocks (Fig. 8, Fig. S27).
572 The proportional contribution of parental alleles towards increased trait
573 values varied between traits, within treatment blocks and throughout plant
574 development. For example, B100 alleles contributed to increased trait values for all
575 traits other than WUE_{ratio} in the water-limited environment and the $WUE_{residual}$
576 across both treatment blocks (Fig. 9). Alternatively, the contributions of the A10
577 alleles proportionally increased the $WUE_{residual}$ value early and then again late in
578 plant development relative to those inherited from the B100 parent. The influence
579 of A10 alleles on the WUE_{ratio} was also greater their B100 counterpart under water-
580 limited conditions early in plant development.
581
582 **DISCUSSION**

Figure 9. The proportional contribution of parental alleles to increased trait values depend upon trait, environmental water content and plant developmental stage.
Alleles derived from the B100 parent contribute a greater proportional of additive genetic variance to plant size, water use and TE model fit in both well-watered and water-limited conditions than their A10 allelic counterparts. Both the WUE ratio and TE model residual traits exhibit dynamic behavior where A10 alleles contribute either greater or close to equal proportions of additive genetic variance early and late in plant development. A) The contribution of parental alleles in the water-limited treatment block. B) The contribution of parental alleles in the water-limited treatment block.

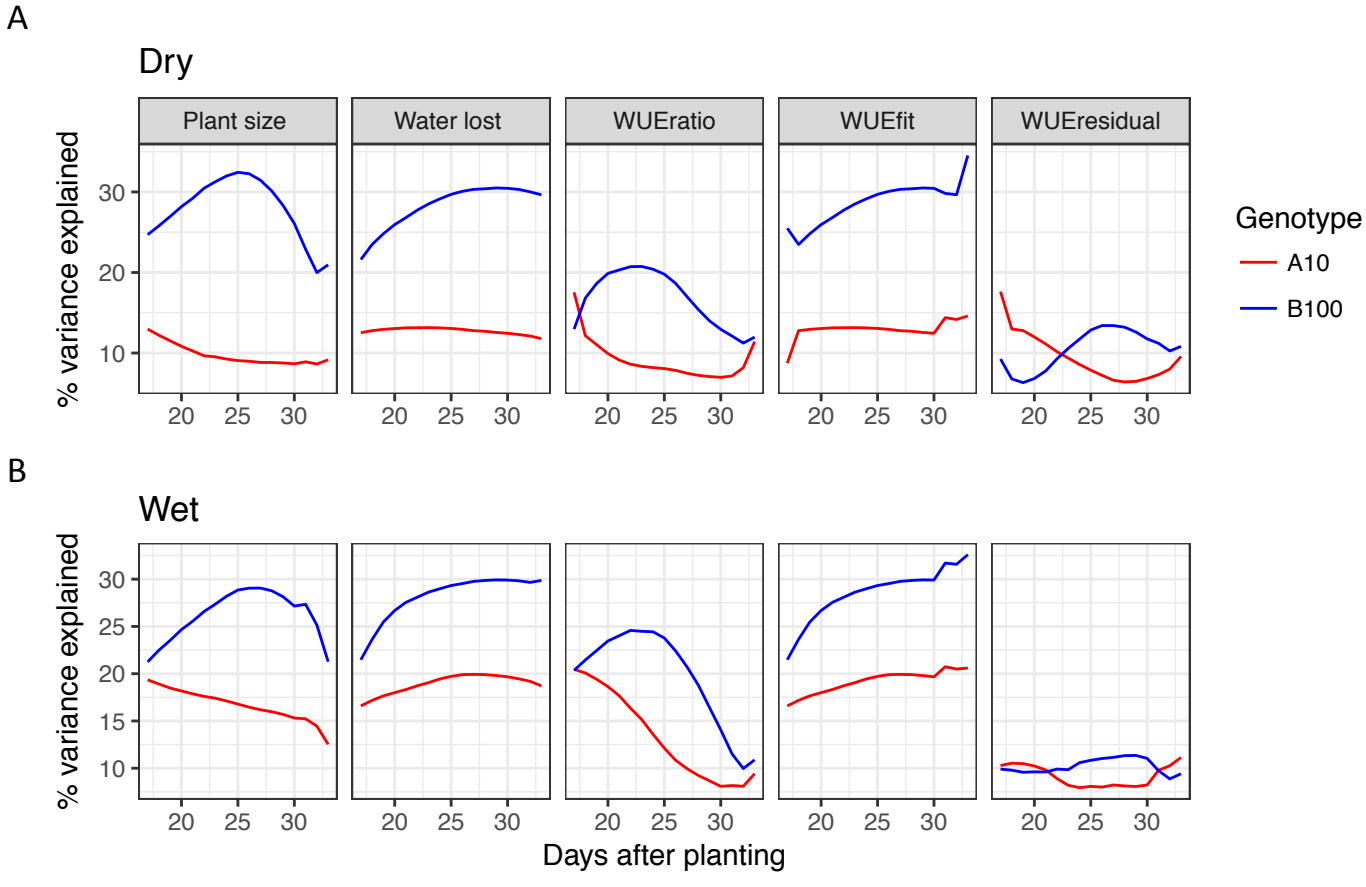

583 The objectives of this study were to utilize technological advances in high-
584 throughput phenotyping (Chen et al., 2014; Fahlgren et al., 2015; Granier et al.,
585 2006; Pereyra-Irujo et al., 2012; Reuzeau et al., 2006; Sadok et al., 2007; Tisné et al.,
586 2013; Walter et al., 2007) to characterize the genetic architecture of water use
587 efficiency and how this architecture responds to water-limitation in an experimental
588 C_4 grass model system. Although considerable efforts have been made to
589 characterize these processes in *Arabidopsis thaliana*, C_3 grass crops and other
590 species (Ruggiero et al., 2017) this represents the first study performed on an
591 annual C_4 grass RIL population. These efforts enabled us to identify genetic loci that
592 contribute to differential biomass accumulation given water use in a well-watered
593 and water-limited environment. Our findings suggest that the major genetic
594 components associated with plant size, water use and water use efficiency exhibit
595 pleiotropic behavior and that the magnitude of their allelic effects is dependent
596 upon environment and developmental stage. We used two complementary
597 approaches to define traits, and our analysis confirmed that the genetic architecture
598 was similar with both approaches. We show that the loci controlling biomass
599 accumulation can be roughly divided into two groups: those that control the amount
600 of water used to create biomass (WUE_{fit}) and those that control how efficiently that
601 water is used ($WUE_{residual}$). The results from this study indicate that alleles from
602 both domesticated foxtail millet and a species representative of its wild progenitor
603 contribute to maximal vegetative biomass yield or water use efficiency grown in
604 environments with different watering regimes. In addition, we highlight aspects of
605 our experimental design and analysis that could be improved in future studies.
606
607 *The genetic architecture of plant size, water use, water use efficiency and the*
608 *relationship between these traits*
609 Within the A10 x B100 *Setaria* RIL population, plant size, water use and the
610 relationship between these two variables are unique polygenic traits whose values
611 are all likely influenced by greater than 10 loci. Four QTL located on 2@96, 5@106,
612 7@99 and 9@36 exhibit strong pleiotropic influence across this suite of traits, the
613 relative magnitude of each is dependent upon growth environment and

614 developmental time point. Despite strong correlation between plant size and water
615 use we successfully identified genetic architectures distinct to each trait. This was
616 achieved by modeling plant size as a function of water use and examining the
617 resulting values of the model fit (plant size given water use) and deviations from
618 this relationship (residual of plant size given water use). This linear modeling
619 approach has been used much less frequently in the literature (Lopez et al., 2015;
620 Nakhforoosh et al., 2016) than the more commonly used WUE_{ratio} (Adiredjo et al.,
621 2014; Honsdorf et al., 2014; Aparna et al., 2015; Fahlgren et al., 2015; Lopez et al.,
622 2015). While the genetic architectures associated with the WUE_{ratio} and $WUE_{residual}$
623 in this population are closely related (Fig. 7), $WUE_{residual}$ exhibits substantial
624 heritability and is less correlated with plant size than the WUE_{ratio} (Fig. S6 Fig. S10),
625 making it a more desirable metric.
626 By examining the model based components of WUE with function valued
627 single marker scan QTL analysis that accounts for multiple hypothesis testing across
628 time points (Kwak et al., 2016), we were able to partition the four major pleiotropic
629 QTL into the genetic components on 2@96, 7@99 and 9@36, which control plant
630 size given water use (WUE_{fit}) and those on 2@96 and 5@109 that contribute to
631 deviations from this relationship ($WUE_{residual}$). This result suggests that QTL
632 associated with WUE_{fit} (7@99 and 9@36) potentially control the development of
633 transpiring plant biomass whereas the QTL associated with the $WUE_{residual}$ and
634 WUE_{ratio} (2@96 and 5@109) influence production of non-transpiring tissues or
635 biological processes not directly related to transpiration. This conclusion is in
636 accordance with the results of other studies performed on this population which
637 demonstrate that these loci are largely pleiotropic (Mauro-Herrera and Doust,
638 2016), although the loci on 2@96 and 5@100 substantially influence plant height
639 (Feldman et al., 2017) and stem biomass, whereas those on 7 and 9 are not
640 associated with the accumulation of stem material (Banan et al., 2017).
641 Our study also identified many smaller effect QTL which influence biomass,
642 water use and WUE traits. The B100 parental allele contributes substantial positive
643 (3@48, 4@52, 6@65, 9@127) and negative (7@34, 7@53) effects on all traits,
644 whereas QTL on 2@11, 2@113, 5@79 and 5@95 contribute either to plant

645 size/WUE_{ratio}/$WUE_{residual}$ ratio to a greater degree than on plant size/water
646 loss/WUE_{fit}.
647 Roughly two thirds of the QTL associated with trait plasticity as a response to
648 water availability (difference or relative difference between treatment blocks) were
649 also identified as being associated with the cumulative traits within both treatment
650 blocks. This observation indicates that in many cases, soil water content influences
651 the temporal dynamics of the allelic effects by differential progression through
652 developmental processes that share similar genetic components (Feldman et al.,
653 2017). This study identifies several QTL (3@48, 7@34 and 9@127) associated with
654 genotype by environment traits which also exhibit significant influence on multiple
655 plant traits within a single treatment block. This provides relatively strong evidence
656 that these QTL have pleiotropic influence on size and water use related traits in an
657 environment specific manner. In contrast, QTL identified only by mapping on the
658 difference or relative difference of the traits between each environment are largely
659 specific to individual traits.
660 Evidence from this study supports an evolutionary genetic model where the
661 majority of QTL associated with the measured traits exhibit conditional neutrality
662 across both soil water potentials examined. Although all traits other than plant size
663 sometimes exhibit opposite directional effects across treatment blocks, the evidence
664 supporting a model of antagonistic pleiotropy is weak. When identified, QTL
665 exhibiting opposite directional effects within individual treatment blocks were
666 limited to short periods of experimental time and are characterized by negligible
667 relative effects during these time points. The contributions of alleles from both
668 parental lines contribute to increased WUE irrespective of soil water potential,
669 suggesting that neither parent was optimized for WUE. For example, alleles from the
670 A10 parent contribute a greater proportion of additive genetic variance to increased
671 WUE during early development in both well-watered and water-limited
672 environments, (particularly given the $WUE_{residual}$ derivation of WUE) whereas the
673 alleles derived from the B100 parent have greater affect on a majority of the
674 measured traits throughout the time course. The contribution of alleles of both
675 parents to water use efficiency is expected given earlier study performed on the

676 same platform where parental lines showed similar WUE under water-limited
677 conditions (Fahlgren et al., 2015).
678
679 *Considerations when measuring plant size, water use and WUE*
680 As observed in many other studies (Chen et al., 2012; Fahlgren et al., 2015;
681 Ge et al., 2016; Golzarian et al., 2011; Honsdorf et al., 2014; Lopez et al., 2015;
682 Parent et al., 2015), relative plant side-view pixel area provided a robust and
683 accurate proximity measurement of plant biomass. Although incorporation of
684 additional plant architectural features can improve estimates of this relationship
685 (Parent et al., 2015), our results indicate that caution should be taken as to not over
686 fit models on ground truth data collected exclusively at the end of the experiment as
687 was performed in this study (Fig. S1).
688 Automated or manual gravimetric measurement of pot weight has proven to
689 be a reliable estimator of plant transpiration but only if the evaporative loss of
690 moisture from soil can be accounted for. Results presented in this study indicate
691 that inclusion of empty pots (or pots that contain plastic plants (Parent et al., 2015)
692 or fabric wicks (Halperin et al., 2017)) is an appropriate empirical method to
693 estimate the experimental time point at which transpiration contributes
694 meaningfully to total pot evapotranspiration (Coupel-Ledru et al., 2016; Lopez et al.,
695 2015; Pereyra-Irujo et al., 2012). Estimation of evapotranspiration after this critical
696 time point has been effectively used by several other groups to identify and
697 eliminate confounding data points collected early during similar experiments
698 (Vasseur et al., 2014; Coupel-Ledru et al., 2016; Ge et al., 2016). Our findings
699 indicate that subtraction of empty pot weight (as performed by (Pereyra-Irujo et al.,
700 2012; Parent et al., 2015; Coupel-Ledru et al., 2016)) may overcorrect for
701 evaporation at early experimental time points even after the point at which plant
702 transpiration contributes substantially to total pot water loss. Although not applied
703 during this experiment, utilization of plastic covering to shield pots from
704 evaporative moisture loss in combination with the approaches discussed above may
705 improve the ability to unambiguously quantify plant transpiration (Aparna et al.,
706 2015; Coupel-Ledru et al., 2016; Ellsworth et al., 2017; Granier et al., 2006; Halperin

707 et al., 2017; Vasseur et al., 2014). In this study, the contribution of plant biomass to
708 overall pot weight was not accounted for during the estimation of plant water use.
709 Although the contribution of plant biomass to pot weight in most experiments
710 performed using *Arabidopsis thaliana* is negligible (Tisné et al., 2010), plant biomass
711 within this *Setaria* RIL population accounted for 12-18% of total average pot water
712 content by the end of the experiment (Fig. S4). Our inability to account for this
713 growth has the undesirable effect of systematically decreasing the soil water
714 content of larger genotypes, although in practice this small change in soil water
715 potential likely has minimal impact on transpiration dynamics of the plants.
716 Strong correlation between plant size and water use was observed in spite of
717 the fact that these traits can potentially be controlled by different physiological
718 mechanisms. A similar trend has also been described in experiments designed to
719 study water use efficiency in *Arabidopsis thaliana*, apple and wheat (Lopez et al.,
720 2015; Nakhforoosh et al., 2016; Schoppach et al., 2016; Parent et al., 2015; Vasseur
721 et al., 2014). The magnitude of this correlation is likely inflated in this study due to
722 the large differences in size between parental lines and segregants within the A10 x
723 B100 RIL population. Future studies aimed at investigating the genetic basis of
724 water use efficiency can attenuate this correlation by selecting parental lines of
725 similar size and flowering times that differ in their rates of transpiration within
726 environments of interest.
727
728 **CONCLUSIONS**
729 This study leverages recent advances in high-throughput phenotyping and
730 quantitative genetics to identify the genetic loci associated with plant size, water use
731 and water use efficiency in an interspecific RIL population of the model C_4 grass
732 *Setaria*. Our findings indicate that these traits are highly heritable and largely
733 polygenic, although the effects of four major pleiotropic QTL account for a
734 substantial proportion of the variance observed within each trait. Contribution of
735 parental alleles from both the domesticated and wild progenitor lines contribute to
736 maximization of these characteristics. Overall, the underlying genetic architecture of
737 each of these processes is distinct and substantially influenced by soil water content

738 as well as plant developmental stage. In addition, several aspects of our
739 experimental design which could be improved to obtain a better understanding of
740 the genetic components that underlie plant size, water use and water use efficiency
741 in future high-throughput phenotyping studies.
742
743 **REFERENCE**

744 **Adiredjo AL, Navaud O, Muños S, Langlade NB, Lamaze T, Grieu P** (2014)
745 Genetic Control of Water Use Efficiency and Leaf Carbon Isotope
746 Discrimination in Sunflower (Helianthus annuus L.) Subjected to Two
747 Drought Scenarios. PLoS ONE **9**: e101218

748 **Aparna K, Nepolean T, Srivastsava RK, Kholová J, Rajaram V, Kumar S, Rekha**
749 **B, Senthilvel S, Hash CT, Vadez V** (2015) Quantitative trait loci associated
750 with constitutive traits control water use in pearl millet [*Pennisetum*
751 *glaucum* (L.) R. Br.]. Plant Biol **17**: 1073–1084

752 **Assouline S, Or D** (2013) Plant Water Use Efficiency over Geological Time –
753 Evolution of Leaf Stomata Configurations Affecting Plant Gas Exchange. PLoS
754 ONE **8**: e67757

755 **Bacon M** (2009) Water Use Efficiency in Plant Biology. John Wiley & Sons, New
756 York, NY

757 **Banan D, Paul R, Feldman MJ, Holmes M, Schlake H, Baxter I, Leakey ADB**
758 (2017) High fidelity detection of crop biomass QTL from low-cost imaging in
759 the field. doi: 10.1101/150144

760 **Bates D, Mächler M, Bolker B, Walker S** (2015) Fitting Linear Mixed-Effects
761 Models Using lme4. J Stat Softw. doi: 10.18637/jss.v067.i01

762 **Bennetzen JL, Schmutz J, Wang H, Percifield R, Hawkins J, Pontaroli AC, Estep**
763 **M, Feng L, Vaughn JN, Grimwood J, et al** (2012) Reference genome
764 sequence of the model plant Setaria. Nat Biotechnol **30**: 555–561

765 **Blatt MR** (2000) Cellular Signaling and Volume Control in Stomatal Movements in
766 Plants. Annu Rev Cell Dev Biol **16**: 221–241

767 **Blum A** (2009) Effective use of water (EUW) and not water-use efficiency (WUE) is
768 the target of crop yield improvement under drought stress. Field Crops Res
769 **112**: 119–123

770 **Boutraa T** (2010) Improvement of Water Use Efficiency in Irrigated Agriculture: A
771 Review. J Agron **9**: 1–8

Boyer JS (1982) Plant Productivity and Environment. Science **218**: 443–448

Bozdogan H (1987) Model selection and Akaike's Information Criterion (AIC): The general theory and its analytical extensions. Psychometrika **52**: 345–370

Brodribb TJ, Feild TS, Jordan GJ (2007) Leaf Maximum Photosynthetic Rate and Venation Are Linked by Hydraulics. PLANT Physiol **144**: 1890–1898

Brodribb TJ, McAdam SAM, Jordan GJ, Feild TS (2009) Evolution of stomatal responsiveness to CO2 and optimization of water-use efficiency among land plants. New Phytol **183**: 839–847

Broman KW, Wu H, Sen S, Churchill GA (2003) R/qtl: QTL mapping in experimental crosses. Bioinformatics **19**: 889–890

Brutnell TP, Wang L, Swartwood K, Goldschmidt A, Jackson D, Zhu X-G, Kellogg E, Van Eck J (2010) Setaria viridis: A Model for C4 Photosynthesis. Plant Cell **22**: 2537–2544

Carmo-Silva AE, Francisco A, Powers SJ, Keys AJ, Ascensao L, Parry MAJ, Arrabaca MC (2009) Grasses of different C4 subtypes reveal leaf traits related to drought tolerance in their natural habitats: Changes in structure, water potential, and amino acid content. Am J Bot **96**: 1222–1235

Chambers JM, Hastie T, eds (1992) Statistical models in S. Wadsworth & Brooks/Cole Advanced Books & Software, Pacific Grove, Calif

Chaves MM (1991) Effects of Water Deficits on Carbon Assimilation. J Exp Bot **42**: 1–16

Chen D, Neumann K, Friedel S, Kilian B, Chen M, Altmann T, Klukas C (2014) Dissecting the Phenotypic Components of Crop Plant Growth and Drought Responses Based on High-Throughput Image Analysis. Plant Cell Online **26**: 4636–4655

Chen J, Chang SX, Anyia AO (2012) Quantitative trait loci for water-use efficiency in barley (Hordeum vulgare L.) measured by carbon isotope discrimination under rain-fed conditions on the Canadian Prairies. Theor Appl Genet **125**: 71–90

Condon AG (2004) Breeding for high water-use efficiency. J Exp Bot **55**: 2447–2460

Condon AG, Richards RA, Rebetzke GJ, Farquhar GD (2002) Improving Intrinsic Water-Use Efficiency and Crop Yield. Crop Sci **42**: 122–131

Coupel-Ledru A, Lebon E, Christophe A, Gallo A, Gago P, Pantin F, Doligez A, Simonneau T (2016) Reduced nighttime transpiration is a relevant breeding

target for high water-use efficiency in grapevine. Proc Natl Acad Sci **113**: 8963–8968

Davies WJ, Bennett MJ (2015) Achieving more crop per drop. Nat Plants **1**: 15118

Des Marais DL, Hernandez KM, Juenger TE (2013) Genotype-by-Environment Interaction and Plasticity: Exploring Genomic Responses of Plants to the Abiotic Environment. Annu Rev Ecol Evol Syst **44**: 5–29

Des Marais DL, Razzaque S, Hernandez KM, Garvin DF, Juenger TE (2016) Quantitative trait loci associated with natural diversity in water-use efficiency and response to soil drying in Brachypodium distachyon. Plant Sci **251**: 2–11

Devos KM, Wang ZM, Beales J, Sasaki T, Gale MD (1998) Comparative genetic maps of foxtail millet (Setaria italica) and rice (Oryza sativa). Theor Appl Genet **96**: 63–68

Easlon HM, Nemali KS, Richards JH, Hanson DT, Juenger TE, McKay JK (2014) The physiological basis for genetic variation in water use efficiency and carbon isotope composition in Arabidopsis thaliana. Photosynth Res **119**: 119–129

Edwards CE, Ewers BE, McClung CR, Lou P, Weinig C (2012) Quantitative Variation in Water-Use Efficiency across Water Regimes and Its Relationship with Circadian, Vegetative, Reproductive, and Leaf Gas-Exchange Traits. Mol Plant **5**: 653–668

Ellsworth PZ, Ellsworth PV, Cousins AB (2017) Relationship of leaf oxygen and carbon isotopic composition with transpiration efficiency in the C4 grasses Setaria viridis and Setaria italica. J Exp Bot **68**: 3513–3528

Escalona JM, TomàS M, Martorell S, Medrano H, Ribas-Carbo M, Flexas J (2012) Carbon balance in grapevines under different soil water supply: importance of whole plant respiration: Carbon balance in grapevine. Aust J Grape Wine Res **18**: 308–318

Evans RG, Sadler EJ (2008) Methods and technologies to improve efficiency of water use: INCREASING WATER USE EFFICIENCIES. Water Resour Res. doi: 10.1029/2007WR006200

Fahlgren N, Feldman M, Gehan MA, Wilson MS, Shyu C, Bryant DW, Hill ST, McEntee CJ, Warnasooriya SN, Kumar I, et al (2015) A Versatile Phenotyping System and Analytics Platform Reveals Diverse Temporal Responses to Water Availability in Setaria. Mol Plant **8**: 1520–1535

841 **Farquhar GD, Hubick KT, Condon AG, Richards RA** (1989) Carbon Isotope
842 Fractionation and Plant Water-Use Efficiency. *In* PW Rundel, JR Ehleringer,
843 KA Nagy, eds, Stable Isot. Ecol. Res. Springer New York, New York, NY, pp 21–
844 40

845 **Feldman MJ, Paul RE, Banan D, Barrett JF, Sebastian J, Yee M-C, Jiang H, Lipka**
846 **AE, Brutnell TP, Dinneny JR, et al** (2017) Time dependent genetic analysis
847 links field and controlled environment phenotypes in the model C4 grass
848 Setaria. PLOS Genet **13**: e1006841

849 **Fleury D, Jefferies S, Kuchel H, Langridge P** (2010) Genetic and genomic tools to
850 improve drought tolerance in wheat. J Exp Bot **61**: 3211–3222

851 **Flood PJ, Harbinson J, Aarts MGM** (2011) Natural genetic variation in plant
852 photosynthesis. Trends Plant Sci **16**: 327–335

853 **Franks PJ, Farquhar GD** (2006) The Mechanical Diversity of Stomata and Its
854 Significance in Gas-Exchange Control. PLANT Physiol **143**: 78–87

855 **Ge Y, Bai G, Stoerger V, Schnable JC** (2016) Temporal dynamics of maize plant
856 growth, water use, and leaf water content using automated high throughput
857 RGB and hyperspectral imaging. Comput Electron Agric **127**: 625–632

858 **Golzarian MR, Frick RA, Rajendran K, Berger B, Roy S, Tester M, Lun DS** (2011)
859 Accurate inference of shoot biomass from high-throughput images of cereal
860 plants. Plant Methods **7**: 2

861 **Granier C, Aguirrezabal L, Chenu K, Cookson SJ, Dauzat M, Hamard P, Thioux J-**
862 **J, Rolland G, Bouchier-Combaud S, Lebaudy A, et al** (2006) PHENOPSIS, an
863 automated platform for reproducible phenotyping of plant responses to soil
864 water deficit in *Arabidopsis thaliana* permitted the identification of an
865 accession with low sensitivity to soil water deficit. New Phytol **169**: 623–635

866 **Gregory PJ, George TS** (2011) Feeding nine billion: the challenge to sustainable
867 crop production. J Exp Bot **62**: 5233–5239

868 **Halperin O, Gebremedhin A, Wallach R, Moshelion M** (2017) High-throughput
869 physiological phenotyping and screening system for the characterization of
870 plant-environment interactions. Plant J **89**: 839–850

871 **Hamdy A, Ragab R, Scarascia-Mugnozza E** (2003) Coping with water scarcity:
872 water saving and increasing water productivity. Irrig Drain **52**: 3–20

873 **Hetherington AM, Woodward FI** (2003) The role of stomata in sensing and driving
874 environmental change. Nature **424**: 901–908

875 **Holloway-Phillips M-M, Brodribb TJ** (2011) Contrasting hydraulic regulation in
876 closely related forage grasses: implications for plant water use. Funct Plant
877 Biol **38**: 594

878 **Honsdorf N, March TJ, Berger B, Tester M, Pillen K** (2014) High-Throughput
879 Phenotyping to Detect Drought Tolerance QTL in Wild Barley Introgression
880 Lines. PLoS ONE **9**: e97047

881 **Huang P, Shyu C, Coelho CP, Cao Y, Brutnell TP** (2016) Setaria viridis as a Model
882 System to Advance Millet Genetics and Genomics. Front Plant Sci. doi:
883 10.3389/fpls.2016.01781

884 **Huxman TE, Smith MD, Fay PA, Knapp AK, Shaw MR, Loik ME, Smith SD, Tissue**
885 **DT, Zak JC, Weltzin JF, et al** (2004) Convergence across biomes to a
886 common rain-use efficiency. Nature **429**: 651–654

887 **Kenney AM, McKay JK, Richards JH, Juenger TE** (2014) Direct and indirect
888 selection on flowering time, water-use efficiency (WUE, δ13C), and WUE
889 plasticity to drought in Arabidopsis thaliana. Ecol Evol **4**: 4505–4521

890 **Kwak I-Y, Moore CR, Spalding EP, Broman KW** (2016) Mapping Quantitative Trait
891 Loci Underlying Function-Valued Traits Using Functional Principal
892 Component Analysis and Multi-Trait Mapping. G3amp58
893 GenesGenomesGenetics **6**: 79–86

894 **Lawson T, Blatt MR** (2014) Stomatal Size, Speed, and Responsiveness Impact on
895 Photosynthesis and Water Use Efficiency. PLANT Physiol **164**: 1556–1570

896 **Lawson T, von Caemmerer S, Baroli I** (2010) Photosynthesis and Stomatal
897 Behaviour. *In* UE Lüttge, W Beyschlag, B Büdel, D Francis, eds, Prog. Bot. 72.
898 Springer Berlin Heidelberg, Berlin, Heidelberg, pp 265–304

899 **Lawson T, Kramer DM, Raines CA** (2012) Improving yield by exploiting
900 mechanisms underlying natural variation of photosynthesis. Curr Opin
901 Biotechnol **23**: 215–220

902 **Legendre P** (2014) lmodel2: Model II Regression. R package version 1.7-2.

903 **Li P, Brutnell TP** (2011) Setaria viridis and Setaria italica, model genetic systems
904 for the Panicoid grasses. J Exp Bot **62**: 3031–3037

905 **Lopez G, Pallas B, Martinez S, Lauri P-É, Regnard J-L, Durel C-É, Costes E** (2015)
906 Genetic Variation of Morphological Traits and Transpiration in an Apple Core
907 Collection under Well-Watered Conditions: Towards the Identification of
908 Morphotypes with High Water Use Efficiency. PLOS ONE **10**: e0145540

909 **Lowry DB, Logan TL, Santuari L, Hardtke CS, Richards JH, DeRose-Wilson LJ,**
910 **McKay JK, Sen S, Juenger TE** (2013) Expression Quantitative Trait Locus
911 Mapping across Water Availability Environments Reveals Contrasting
912 Associations with Genomic Features in Arabidopsis. Plant Cell **25**: 3266–
913 3279

914 **Martre P, Cochard H, Durand J-L** (2001) Hydraulic architecture and water flow in
915 growing grass tillers (Festuca arundinacea Schreb.). Plant Cell Environ **24**:
916 65–76

917 **Mauro-Herrera M, Doust AN** (2016) Development and Genetic Control of Plant
918 Architecture and Biomass in the Panicoid Grass, Setaria. PLOS ONE **11**:
919 e0151346

920 **Mojica JP, Mullen J, Lovell JT, Monroe JG, Paul JR, Oakley CG, McKay JK** (2016)
921 Genetics of water use physiology in locally adapted Arabidopsis thaliana.
922 Plant Sci **251**: 12–22

923 **Monteith JL** (1993) The exchange of water and carbon by crops in a mediterranean
924 climate. Irrig Sci. doi: 10.1007/BF00208401

925 **Morison JI., Baker N., Mullineaux P., Davies W.** (2008) Improving water use in
926 crop production. Philos Trans R Soc B Biol Sci **363**: 639–658

927 **Nakhforoosh A, Bodewein T, Fiorani F, Bodner G** (2016) Identification of Water
928 Use Strategies at Early Growth Stages in Durum Wheat from Shoot
929 Phenotyping and Physiological Measurements. Front Plant Sci. doi:
930 10.3389/fpls.2016.01155

931 **Parent B, Shahinnia F, Maphosa L, Berger B, Rabie H, Chalmers K, Kovalchuk A,**
932 **Langridge P, Fleury D** (2015) Combining field performance with controlled
933 environment plant imaging to identify the genetic control of growth and
934 transpiration underlying yield response to water-deficit stress in wheat. J
935 Exp Bot **66**: 5481–5492

936 **Pater D, Mullen JL, McKay JK, Schroeder JI** (2017) Screening for Natural Variation
937 in Water Use Efficiency Traits in a Diversity Set of Brassica napus L. Identifies
938 Candidate Variants in Photosynthetic Assimilation. Plant Cell Physiol **58**:
939 1700–1709

940 **Penman H, Schofield R** (1951) Some physical aspects of assimilation and
941 transpiration. Carbon Dioxide Fixat. Photosynth. 5:

942 **Pereyra-Irujo GA, Gasco ED, Peirone LS, Aguirrezábal LAN** (2012) GlyPh: a low-
943 cost platform for phenotyping plant growth and water use. Funct Plant Biol
944 **39**: 905

945 **Premachandra GS, Hahn DT, Axtell JD, Joly RJ** (1994) Epicuticular wax load and
946 water-use efficiency in bloomless and sparse-bloom mutants of Sorghum
947 bicolor L. Environ Exp Bot **34**: 293–301

948 **Reuzeau C, Frankard V, Hatzfeld Y, Sanz A, Van Camp W, Lejeune P, De Wilde C,**
949 **Lievens K, de Wolf J, Vranken E, et al** (2006) Traitmill™: a functional
950 genomics platform for the phenotypic analysis of cereals. Plant Genet Resour
951 Charact Util **4**: 20–24

952 **Ruggiero A, Punzo P, Landi S, Costa A, Van Oosten M, Grillo S** (2017) Improving
953 Plant Water Use Efficiency through Molecular Genetics. Horticulturae **3**: 31

954 **Ryan AC, Dodd IC, Rothwell SA, Jones R, Tardieu F, Draye X, Davies WJ** (2016)
955 Gravimetric phenotyping of whole plant transpiration responses to
956 atmospheric vapour pressure deficit identifies genotypic variation in water
957 use efficiency. Plant Sci **251**: 101–109

958 **Sack L, Holbrook NM** (2006) LEAF HYDRAULICS. Annu Rev Plant Biol **57**: 361–381

959 **Sadok W, Naudin P, Boussuge B, Muller B, Welcker C, Tardieu F** (2007) Leaf
960 growth rate per unit thermal time follows QTL-dependent daily patterns in
961 hundreds of maize lines under naturally fluctuating conditions. Plant Cell
962 Environ **30**: 135–146

963 **Saha P, Sade N, Arzani A, Rubio Wilhelmi M del M, Coe KM, Li B, Blumwald E**
964 (2016) Effects of abiotic stress on physiological plasticity and water use of
965 Setaria viridis (L.). Plant Sci **251**: 128–138

966 **Schoppach R, Taylor JD, Majerus E, Claverie E, Baumann U, Suchecki R, Fleury**
967 **D, Sadok W** (2016) High resolution mapping of traits related to whole-plant
968 transpiration under increasing evaporative demand in wheat. J Exp Bot **67**:
969 2847–2860

970 **Seibt U, Rajabi A, Griffiths H, Berry JA** (2008) Carbon isotopes and water use
971 efficiency: sense and sensitivity. Oecologia **155**: 441–454

972 **Stanhill G** (1986) Water Use Efficiency. Adv. Agron. Elsevier, pp 53–85

973 **Stewart G, Turnbull M, Schmidt S, Erskine P** (1995) 13C Natural Abundance in
974 Plant Communities Along a Rainfall Gradient: a Biological Integrator of Water
975 Availability. Aust J Plant Physiol **22**: 51

976 **Tardieu F** (2013) Plant response to environmental conditions: assessing potential
977 production, water demand, and negative effects of water deficit. Front
978 Physiol. doi: 10.3389/fphys.2013.00017

979 **Tisné S, Schmalenbach I, Reymond M, Dauzat M, Pervent M, Vile D, Granier C**
980 (2010) Keep on growing under drought: genetic and developmental bases of
981 the response of rosette area using a recombinant inbred line population: Leaf
982 development and drought stress. Plant Cell Environ **33**: 1875–1887

983 **Tisné S, Serrand Y, Bach L, Gilbault E, Ben Ameur R, Balasse H, Voisin R,**
984 **Bouchez D, Durand-Tardif M, Guerche P, et al** (2013) Phenoscope: an
985 automated large-scale phenotyping platform offering high spatial
986 homogeneity. Plant J **74**: 534–544

987 **Tomás M, Medrano H, Escalona JM, Martorell S, Pou A, Ribas-Carbó M, Flexas J**
988 (2014) Variability of water use efficiency in grapevines. Environ Exp Bot
989 **103**: 148–157

990 **Vasseur F, Bontpart T, Dauzat M, Granier C, Vile D** (2014) Multivariate genetic
991 analysis of plant responses to water deficit and high temperature revealed
992 contrasting adaptive strategies. J Exp Bot **65**: 6457–6469

993 **Walter A, Scharr H, Gilmer F, Zierer R, Nagel KA, Ernst M, Wiese A, Virnich O,**
994 **Christ MM, Uhlig B, et al** (2007) Dynamics of seedling growth acclimation
995 towards altered light conditions can be quantified via GROWSCREEN: a setup
996 and procedure designed for rapid optical phenotyping of different plant
997 species. New Phytol **174**: 447–455

998 **Wang ZM, Devos KM, Liu CJ, Wang RQ, Gale MD** (1998) Construction of RFLP-
999 based maps of foxtail millet, Setaria italica (L.) P. Beauv. Theor Appl Genet
1000 **96**: 31–36

1001 **White TA, Snow VO** (2012) A modelling analysis to identify plant traits for
1002 enhanced water-use efficiency of pasture. Crop Pasture Sci **63**: 63

1003 **Winter K, Aranda J, Holtum JAM** (2005) Carbon isotope composition and water-
1004 use efficiency in plants with crassulacean acid metabolism. Funct Plant Biol
1005 **32**: 381

1006 **Xu Y, This D, Pausch RC, Vonhof WM, Coburn JR, Comstock JP, McCouch SR**
1007 (2009) Leaf-level water use efficiency determined by carbon isotope
1008 discrimination in rice seedlings: genetic variation associated with population
1009 structure and QTL mapping. Theor Appl Genet **118**: 1065–1081

1010 **Zegada-Lizarazu W, Iijima M** (2005) Deep Root Water Uptake Ability and Water
1011 Use Efficiency of Pearl Millet in Comparison to Other Millet Species. Plant
1012 Prod Sci **8**: 454–460

1013 **Zhou Y, Lambrides CJ, Kearns R, Ye C, Fukai S** (2012) Water use, water use
1014 efficiency and drought resistance among warm-season turfgrasses in shallow
1015 soil profiles. Funct Plant Biol **39**: 116

1016 **Zhu C, Yang J, Shyu C** (2017) Setaria Comes of Age: Meeting Report on the Second
1017 International Setaria Genetics Conference. Front Plant Sci. doi:
1018 10.3389/fpls.2017.01562

1019